

RESEARCH ARTICLE

Open Access



# Cyclosporine a directly affects human and mouse b cell migration in vitro by disrupting a HIF-1 $\alpha$ dependent, O<sub>2</sub> sensing, molecular switch

Shannon P Hilchey<sup>1</sup>, Mukta G Palshikar<sup>2</sup>, Jason A Emo<sup>1</sup>, Dongmei Li<sup>3</sup>, Jessica Garigen<sup>3</sup>, Jiong Wang<sup>1</sup>, Eric S Mendelson<sup>1</sup>, Valentina Cipolla<sup>1</sup>, Juilee Thakar<sup>4,5</sup> and Martin S Zand<sup>1,3\*</sup>

## Abstract

**Background:** Hypoxia is a potent molecular signal for cellular metabolism, mitochondrial function, and migration. Conditions of low oxygen tension trigger regulatory cascades mediated via the highly conserved HIF-1 $\alpha$  post-translational modification system. In the adaptive immune response, B cells (Bc) are activated and differentiate under hypoxic conditions within lymph node germinal centers, and subsequently migrate to other compartments. During migration, they traverse through changing oxygen levels, ranging from 1-5% in the lymph node to 5-13% in the peripheral blood. Interestingly, the calcineurin inhibitor cyclosporine A is known to stimulate prolyl hydroxylase activity, resulting in HIF-1 $\alpha$  destabilization and may alter Bc responses directly. Over 60% of patients taking calcineurin immunosuppressant medications have hypo-gammaglobulinemia and poor vaccine responses, putting them at high risk of infection with significantly increased morbidity and mortality.

**Results:** We demonstrate that O<sub>2</sub> tension is a previously unrecognized Bc regulatory switch, altering CXCR4 and CXCR5 chemokine receptor signaling in activated Bc through HIF-1 $\alpha$  expression, and controlling critical aspects of Bc migration. Our data demonstrate that calcineurin inhibition hinders this O<sub>2</sub> regulatory switch in primary human Bc.

**Conclusion:** This previously unrecognized effect of calcineurin inhibition directly on human Bc has significant and direct clinical implications.

**Keywords:** HIF-1 $\alpha$ , Hypoxia, B cells, CXCR4/CXCL12, CXCR5/CXCL13, Chemotaxis

## Background

Calcineurin inhibitors (CNI), such as cyclosporine A (CyA), are used to reduce the risk of allograft rejection in solid organ transplant recipients, and prevent graft-versus-host disease in bone marrow transplantation [1]. One side effect of CNI therapy is reduced antigen-specific

B cell responsiveness, including hypogammaglobulinemia and reduced protective IgG responses to influenza and other vaccinations [2, 3]. This effect has previously been thought to be primarily due to CD4 T cell inhibition [4]. CNI directly inhibit CD4 T cell calcineurin signaling by preventing calcineurin dependent dephosphorylation of the transcription factor NFAT, blocking nuclear translocation, inhibiting IL-2 production and proliferation [4]. In transplant recipients, CNI are thus thought to primarily suppress CD4 T cell help, indirectly causing B cell hypo-responsiveness and depressing antibody production [4]. In contrast, direct effects of CNI on B cell function, in

\*Correspondence: [martin\protect\\_zand@urmc.rochester.edu](mailto:martin\protect_zand@urmc.rochester.edu)

<sup>1</sup>University of Rochester Medical Center, Division of Nephrology, 601 Elmwood Ave., 14642 Rochester, NY, USA

<sup>3</sup>University of Rochester, Clinical and Translational Science Institute, 265 Crittenden Blvd., 14642 Rochester, NY, USA

Full list of author information is available at the end of the article



© The Author(s). 2020 **Open Access** This article is licensed under a Creative Commons Attribution 4.0 International License, which permits use, sharing, adaptation, distribution and reproduction in any medium or format, as long as you give appropriate credit to the original author(s) and the source, provide a link to the Creative Commons licence, and indicate if changes were made. The images or other third party material in this article are included in the article's Creative Commons licence, unless indicated otherwise in a credit line to the material. If material is not included in the article's Creative Commons licence and your intended use is not permitted by statutory regulation or exceeds the permitted use, you will need to obtain permission directly from the copyright holder. To view a copy of this licence, visit <http://creativecommons.org/licenses/by/4.0/>. The Creative Commons Public Domain Dedication waiver (<http://creativecommons.org/publicdomain/zero/1.0/>) applies to the data made available in this article, unless otherwise stated in a credit line to the data.

particular cellular migration, are sparsely described in the literature [5].

Several pieces of evidence suggest that hypoxia may modulate post-germinal center (GC) B cell migration, and that CNI could interfere with this process. Low tissue oxygen ( $O_2$ ) tension ( $\leq 1\%$   $O_2$ ; hypoxia) has emerged as an important immune modulating signal [6–11]. Intriguingly, low  $O_2$  tension occurs in secondary lymphoid organs, particularly in draining lymph nodes (LN) and bone marrow (BM) [12, 13]. Lymphocytes within these organs express hypoxia induced (transcription) factor-1 $\alpha$  (HIF-1 $\alpha$ ) at low  $O_2$  tensions (1% - 4%) [14–16]. It has recently been shown that GC hypoxia itself is important for efficient B cell class switching and antibody production in mouse models [17, 18], directly linking hypoxia to B cell function. Despite these results, the mechanism by which B cell function is directly affected by hypoxia during migration to regions of secondary lymphoid tissues with low oxygen  $O_2$  tension, remains undefined [12, 13].

Although current data support the premise that  $O_2$  tension modulates transcriptome and molecular signaling events in human T [14, 15, 19–21] and lymphoma cells [22–24], the effects of  $O_2$  tension has on B cell responses are largely unknown. We have previously demonstrated that HIF-1 $\alpha$  transcripts are upregulated in both human differentiating B cells in vitro and plasma cells migrating in vivo through peripheral blood to bone marrow post-vaccination [25, 26]. Coordinated migration of B cells between GC, peripheral blood (PB), spleen and BM is critical for the B cell response [27–30], and is modulated in part by CXCR4 [31] and its ligand CXCL12 [27–30], which are known to be regulated by HIF-1 $\alpha$  in other cells [14–16]. CXCR4 signaling is regulated by transcriptional control, protein expression, and receptor internalization [32]. Interestingly, GC B cells have been shown to express surface CXCR4, however, they are unresponsive to CXCL12 signaling [33, 34]. As GC B cells encounter  $O_2$  levels, at times  $< 1\%$ , it is likely that CXCR4 responsiveness is in part controlled by an  $O_2$  dependent post-translational mechanism, independent of CXCR4 transcription, translation or surface expression.

Based on the above data, we hypothesize that changes in  $O_2$  tension as B cells migrate within the GC may directly control the localization and functional activation and differentiation of B cells. This hypothesis is strongly supported by the  $O_2$  dependent regulation of several CXCR4 signaling components, including RGS1, which mediates HIF-1 $\alpha$  induced CXCR4 uncoupling, along with p44/p42 MAPK and MKP-1 [34]. Focal adhesion kinase (FAK) is also critical for CXCR4 dependent migration of B cells [16], and is modulated by  $O_2$  tension in smooth muscle cells [35]. In addition, CNI are known to interact directly and indirectly with the HIF-1 $\alpha$  signaling cascade, and may have a significant role in disrupting the normal

hypoxia-induced regulation of B cell migration. For example, CNI destabilize HIF-1 $\alpha$  in glioma cells by stimulating prolyl hydroxylase activity [36], suggesting CNI have the capacity to disrupt hypoxic responses. Thus, there is also strong support for the additional hypothesis that hypoxia induced pathways are involved in modulation of CXCR4 signaling in B cells and CNI may disrupt these pathways.

In the following study, we demonstrate that migration of human and mouse B cells is regulated by chemokine receptor (CXCR4 and CXCR5) responsiveness via an  $O_2$  sensing molecular switch, controlled by HIF-1 $\alpha$ , which is independent of CXCR4/CXCR5 receptor expression or surface localization. Our data support the hypothesis that B cell migration is modulated by chemokine receptor sensitivity, controlled by stabilization of the master regulator HIF-1 $\alpha$  at low  $O_2$  levels ( $< 4\%$ ), and indeed, we show genetically that HIF-1 $\alpha$  is necessary for this effect. Significantly, CyA destabilizes HIF-1 $\alpha$  in both human and mouse B cells, partially restoring chemokine receptor responsiveness at low  $O_2$  levels. These identical findings in both human and mouse cells may allow for a highly correlated assessment of in vivo immunological responses developing in lymph node and spleen using mouse models, as direct assessments are not possible in humans for anatomical and ethical reasons. Additional unbiased proteomics data suggests a switch in several metabolic processes potentially facilitating migration. This is consistent with the regulation of extracellular matrix and intrinsic apoptosis observed in the proteomic analysis. Transient re-stabilization of HIF-1 $\alpha$  in CyA treated B cells temporarily restores the  $O_2$  dependent molecular switch modulating B cell migration. These novel findings identify a direct, and potentially therapeutically targetable effect of CNI on B cell function, independent of indirect helper T cell effects.

## Results

### Human and mouse B cell chemokine receptor (CXCR4 and CXCR5) hypo-responsiveness is induced by low $O_2$ levels and this correlates with HIF-1 $\alpha$ stabilization

In order to examine B cell CXCR4 and CXCR5 responsiveness at different  $O_2$  levels, we developed a novel, high throughput, in vitro transmigration assay system that combines a 96 well transwell plate format with a rapid luminescent readout of migratory cell numbers. Precise  $O_2$  level control was achieved using two separate C-Chamber  $O_2$  controlled incubator chambers (Biospherix, Parish, NY) to measure cell migration under varying levels of hypoxia. B cells in a developing immune response typically experience 1-4%  $O_2$  within a local draining lymph node. To replicate these conditions, multiple C-Chambers were used to incubate separate chambers in parallel under three different  $O_2$  levels in a single experiment. Thus,  $O_2$  levels from the traditional 37°C, humidified,  $CO_2$  incubator provided 19%  $O_2$ , and two

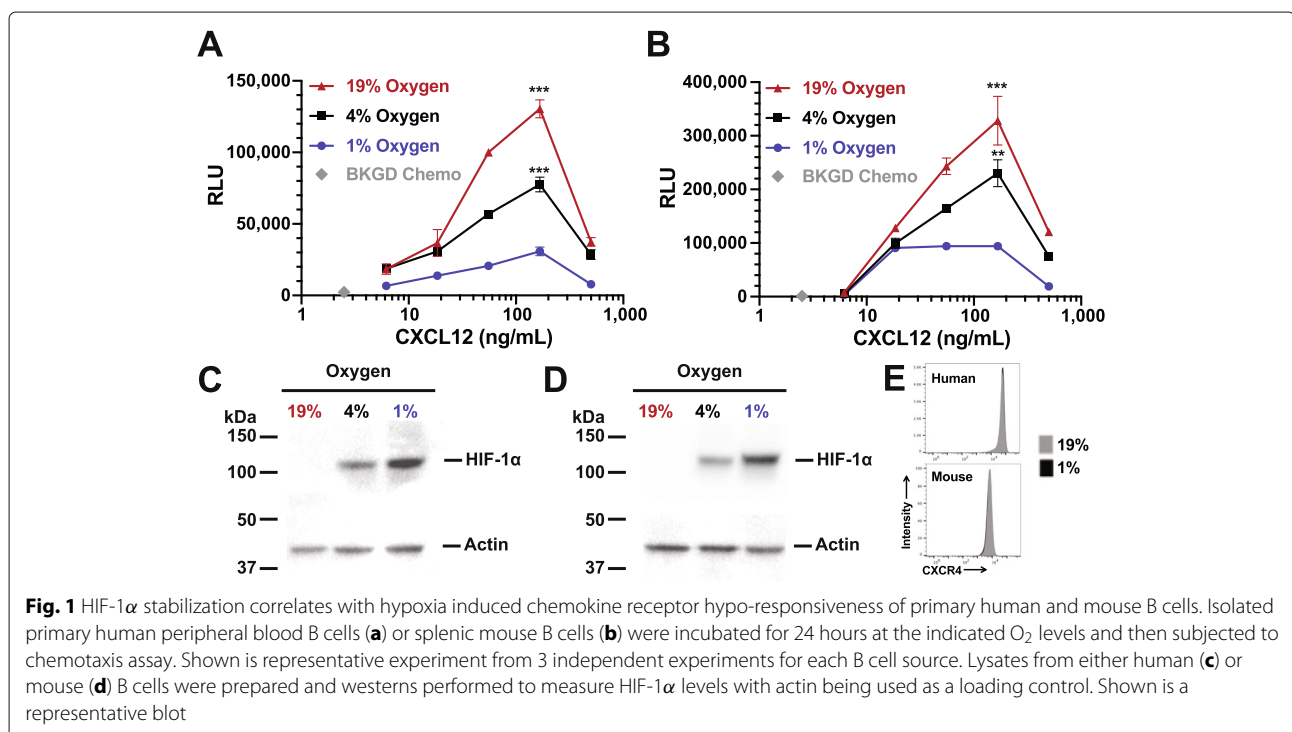
C-chambers within the same incubator provided 1% and 4% O<sub>2</sub>.

We first examined the affect of 1 - 19% O<sub>2</sub> levels on freshly isolated human peripheral blood and murine splenic B cells. Primary human peripheral blood B cells (n=3 donors) incubated at 19% O<sub>2</sub> for 24 hours migrate in responses to CXCL12 or CXCL13 (Fig. 1a and Supplementary Figure 1a). However, CXCL12 and CXCL13 induced human B cell migration was inhibited at O<sub>2</sub> tensions of 1% or 4% O<sub>2</sub>. Mouse B cells exhibited an identical inhibition of chemotaxis at lower O<sub>2</sub> levels (Fig. 1b and Supplementary Figure 1b), with robust chemotaxis to CXCL12 or CXCL13 at 19% O<sub>2</sub>, which decreases with 24 hours of incubation at 1% or 4% O<sub>2</sub>. Importantly, we observed no effect on human or mouse B cell surface CXCR4/CXCR5 expression (Fig. 1e and Supplementary Figure 2c) or viability (Supplementary Figure 2ab) irrespective of O<sub>2</sub> levels. These data strongly suggest that the decrease in chemotaxis is not due to decreased cellular viability or to loss of CXCR4/CXCR5 surface expression. The decreased chemotaxis was highly reproducible and the decreased chemotactic activity observed at lower O<sub>2</sub> levels is highly significant ( $p < 0.001$  for all pairwise comparisons). This finding of virtually identical CXCR4/CXCL12 or CXCR5/CXCL13 chemotaxis in mouse and human B cells suggests a highly conserved regulatory system.

CXCR4 chemokine receptor sensitivity has been shown to be modulated by stabilization of the transcription factor HIF-1 $\alpha$ , which occurs at low O<sub>2</sub> levels in most cells and induces nuclear translocation [6]. Thus, we next performed experiments to confirm HIF-1 $\alpha$  stabilization correlates with CXCR4 or CXCR5 hypo-responsiveness. Figure 1 shows a western blot analysis of HIF-1 $\alpha$  protein levels in nuclear lysates prepared from human peripheral blood B cells Fig. 1c) and mouse splenic B cells (Fig. 1d), incubated at the same O<sub>2</sub> levels used in the chemotaxis assay. Neither human nor mouse B cells incubated at 19% O<sub>2</sub> exhibit detectable levels of HIF-1 $\alpha$  protein in nuclear lysates (Fig. 1cd). Thus there is a negative correlation between nuclear HIF-1 $\alpha$  protein levels and human or mouse B cell chemotactic activity.

**Low O<sub>2</sub> levels induce CXCR4/CXCR5 hypo-responsiveness and HIF-1 $\alpha$  stabilization in RAMOS human B cells**

The quantities of nuclear extracts that can be obtained from primary human or mouse splenic B cells significantly limit comparisons of multiple experimental conditions. Thus, we choose to perform more detailed western and proteomics analysis using the RAMOS human B cell line. First we confirmed that relationship between chemotaxis and HIF-1 $\alpha$  stabilization seen in primary mouse and human cells was recapitulated in RAMOS cells. Identical to what we observed using primary B cells, the RAMOS human B cell line migrates in response to a CXCL12 or



CXCL13 chemokine gradient at 19% O<sub>2</sub> in a dose dependent fashion. In contrast, incubation for 24 hours at 1% or 4% O<sub>2</sub> results in significantly decreased migration for both CXCL12 and CXCL13 gradients (Fig. 2a and Supplementary Figure 1c). As with the primary cells, we also observed no effect on RAMOS cell viability, proliferation or surface CXCR4/CXCR5 expression (Fig. 2d and Supplementary Figure 2ab and c). This was irrespective of O<sub>2</sub> levels, again suggesting that the decrease in chemotaxis is not due to decreased cellular viability and/or proliferation, nor due to loss of chemokine receptor surface expression. In addition to examining viability and proliferation, we also wanted to determine if the low O<sub>2</sub> effects permanently alter the ability of RAMOS cells to respond to a CXCL12 gradient. We incubated RAMOS cells at 1% O<sub>2</sub> levels for 24 hours and then re-exposed the cells to 19% O<sub>2</sub> for 2, 4 or 6 hours and then subjected the cells to our chemotaxis assay. As is evident from Figure 2e RAMOS cells progressively regain the capacity to migrate in response to a CXCL12 gradient through 6 hours of re-exposure to 19% O<sub>2</sub>.

Similar to primary human and mouse cells, western blot analysis of nuclear lysates showed that HIF-1 $\alpha$  protein was barely detectable after incubation of human RAMOS cells at 19% O<sub>2</sub> for 24 hours (Fig. 2b and c). In contrast, levels of HIF-1 $\alpha$  protein increase over time in nuclear lysates when cells are incubated at lower O<sub>2</sub> levels (4% and 1%, a 5.3 and 7.6 fold increase as compared to 19%, respectively), demonstrating O<sub>2</sub> dependent HIF-1 $\alpha$  protein stabilization and nuclear localization.

In addition to HIF-1 $\alpha$  stabilization, HIF-2 $\alpha$  has also been shown to be stabilized upon hypoxic exposure of several different cell types [37, 38], but there is little data in human B cells. We performed a western blot analysis of HIF-2 $\alpha$  protein stabilization in the RAMOS human B cells under varying O<sub>2</sub> conditions. We did not observe any significant HIF-2 $\alpha$  stabilization in the nuclear lysates at low O<sub>2</sub> levels (Supplementary Figure 3). These results suggest that HIF-2 $\alpha$  does not play a significant role in O<sub>2</sub> sensitive human B cell migration within the experimental time frame.

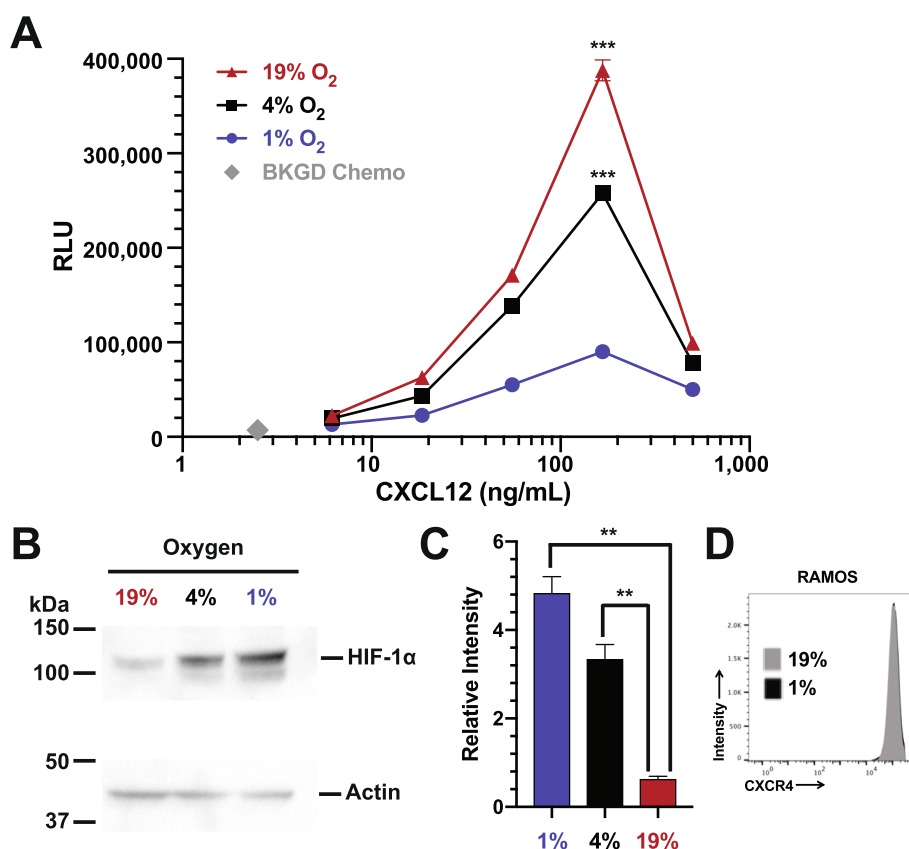


**Fig. 2** HIF-1 $\alpha$  stabilization correlates with hypoxia induced chemokine receptor hypo-responsiveness of the RAMOS B cell line. RAMOS B cells were incubated at the indicated O<sub>2</sub> levels for 24 hours and then subjected to (a) chemotaxis assay or (b) lysates were prepared and westerns performed to measure HIF-1 $\alpha$  levels with actin being used as a loading control. Shown is a representative blot. (c) Quantitation of relative HIF-1 $\alpha$  levels from three separate experiments. \*\*\* $P$ <0.001; \*\* $P$ <0.01

### **HIF-1 $\alpha$ is both necessary and sufficient for CXCR4 hypo-responsiveness**

We hypothesized that HIF-1 $\alpha$  expression is necessary for B cell chemotactic hypo-responsiveness at low O<sub>2</sub> levels, and evaluated this hypothesis using shRNA silencing of HIF-1 $\alpha$ . Stable RAMOS B cell lentiviral transfectants were generated expressing either HIF-1 $\alpha$  shRNA, or a control non-specific shRNA vector and evaluated at the peak chemotaxis dose of CXCL12 (166  $\mu$ g/mL; Fig. 2a). We focused on CXCR4/CXCL12 chemotaxis for the remainder of the manuscript, as we have shown that the O<sub>2</sub>/chemotactic effect is similar when comparing CXCR4 and CXCR5. For simplicity, we analyzed chemotaxis at the peak response (166  $\mu$ g/mL). RAMOS cells expressing HIF-1 $\alpha$  shRNA had increased chemotactic activity at 1% O<sub>2</sub> levels as compared to either the control shRNA transfectants or non-transfected cells (Fig. 3a). As predicted, HIF-1 $\alpha$  protein levels were significantly decreased in HIF-1 $\alpha$  shRNA transfected cells (Fig. 3b and c). These genetic silencing results clearly demonstrate that HIF-1 $\alpha$  expression is necessary for the observed decrease in CXCR4 responsiveness at low O<sub>2</sub> levels.

We also tested the hypothesis that HIF-1 $\alpha$  is sufficient to induce chemotactic hypo-responsiveness at high O<sub>2</sub> levels using a HIF-1 $\alpha$  over-expression system. RAMOS cells were stably transfected with a lentiviral vector expressing either HIF-1 $\alpha$  or a control firefly luciferase. Post-transfection chemotaxis was evaluated at the peak dose of CXCL12 (166  $\mu$ g/mL). As expected, RAMOS cells over-expressing HIF-1 $\alpha$  demonstrated a significant decrease in chemotactic capacity at 19% O<sub>2</sub> as compared to either the untransfected or luciferase expressing RAMOS cells (Fig. 3d). In addition, HIF-1 $\alpha$  protein levels were significantly increased in transfected cells over-expressing the HIF-1 $\alpha$  construct (Fig. 3e and f). These genetic over-expressing results clearly demonstrate that HIF-1 $\alpha$  expression is sufficient to account for the observed decrease in CXCR4 responsiveness at low O<sub>2</sub> levels.

### **Cyclosporine A inhibits hypoxia dependent CXCR4 hypo-responsiveness by destabilizing HIF-1 $\alpha$**

Cyclosporine A (CyA) destabilizes HIF-1 $\alpha$  in glioma cells [36]. We hypothesized that CyA could similarly disrupt B cell HIF-1 $\alpha$  stabilization, altering chemokine-induced B cell migration. Consistent with this hypothesis, and the above data, exposing RAMOS B cells to 1% O<sub>2</sub> inhibits CXCL12 mediated chemotaxis relative to that observed at 19% O<sub>2</sub>. However, treatment with increasing concentrations of CyA progressively increases CXCL12 mediated chemotaxis of RAMOS cells at 1% O<sub>2</sub> (Fig. 4a). These results are preserved across both primary human and mouse B cells, which also exhibit a similar increase in chemotactic activity after treatment with CyA (Fig. 4d and

e). The levels of CyA used in these experiments are physiologically relevant, as serum levels of 10-2000 ng/mL are achieved in vivo in immunosuppressed renal transplant recipients [39].

To assess the correlation between CyA's effect on migration and HIF-1 $\alpha$  stabilization, we performed western blot analysis on RAMOS nuclear lysates over a range of CyA levels. Figure 4b and c demonstrate that treatment of RAMOS cells, with increasing amounts of CyA at 1% O<sub>2</sub> leads to a progressive decrease in HIF-1 $\alpha$  levels. These results again directly link HIF-1 $\alpha$  with chemotactic activity, demonstrating that CyA treatment results in decreased HIF-1 $\alpha$  protein levels with increased CXCR4 responsiveness and chemotaxis, despite the fact that the B cells are incubated at 1% O<sub>2</sub>.

We hypothesize that the observed effect CyA has on B cell chemotaxis is mediated through HIF-1 $\alpha$ . As such, we would anticipate that the HIF shRNA expressing cells would be insensitive to the CyA effect at low O<sub>2</sub> levels. To confirm this hypothesis, we incubated untransfected, control shRNA, or HIF shRNA expressing RAMOS cells at 1% O<sub>2</sub> for 24 hours with or without CyA and then subjected the cells to our chemotaxis assay. As is evident from Fig. 4f both the untransfected and control shRNA expressing cells demonstrated increased chemotactic activity upon treatment with CyA. In contrast, no increase in chemotactic activity was observed with the HIF shRNA cells after treatment with CyA. These results strongly support the hypothesis that CyA alters B cell chemotactic activity directly through modulation of HIF-1 $\alpha$ .

### **Pharmacological stabilization of HIF-1 $\alpha$ at 19% O<sub>2</sub> mimics the effects of low O<sub>2</sub> levels**

The above results strongly suggest that an O<sub>2</sub> sensing molecular switch modulates B cell migration, correlates with and requires HIF-1 $\alpha$  stabilization, and is sensitive to CyA treatment. We thus tested the hypothesis that pharmacologically stabilization of HIF at 19% O<sub>2</sub> would mimic the effect of incubating the cells at low O<sub>2</sub>. We performed experiments stabilizing HIF-1 $\alpha$  at 19% O<sub>2</sub> using the prolyl-4-hydroxylase (PHD) inhibitor dimethylallyl glycine (DMOG). DMOG has been reported to selectively stabilize HIF-1 $\alpha$ , with minimal effects on HIF-2 $\alpha$  [38]. We found that incubation of RAMOS cells with DMOG at 19% O<sub>2</sub> resulted in decreased CXCL12 responsiveness (Fig. 5a), similar to the effect observed at low O<sub>2</sub> levels. DMOG had a similar effect on primary human and mouse B cells (Fig. 5c and d). Western blot analysis (Fig. 5b) of nuclear lysates from RAMOS cells confirms that the CXCL12 chemotactic effects highly correlates with HIF-1 $\alpha$  protein stabilization, even when the cells were incubated at 19% O<sub>2</sub>.

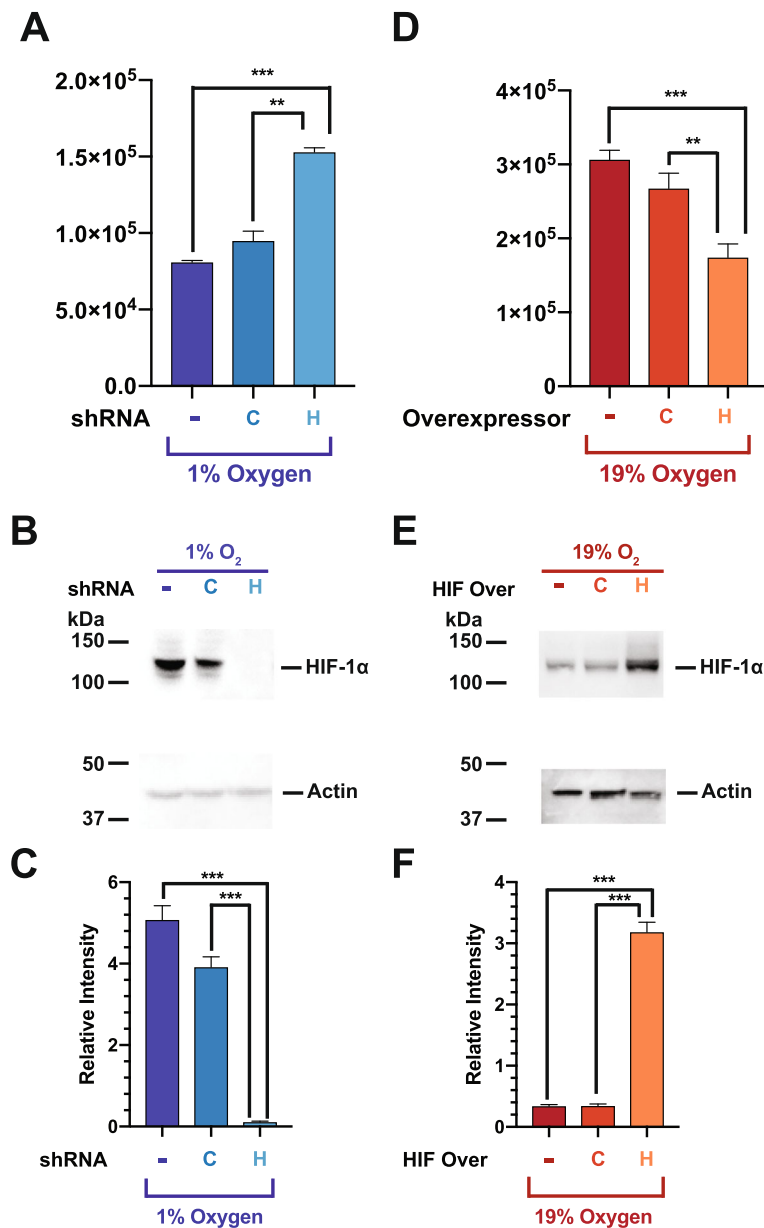


**Fig. 3** HIF-1 $\alpha$  is both necessary and sufficient to induce chemokine receptor hypo-responsiveness. Ramos B cells, stably transfected with lentiviral vectors expressing either HIF-1 $\alpha$  shRNA (H), a scrambled non-specific control sequence shRNA (C) or parental non-transfected Ramos cells (-), were incubated at the indicated O<sub>2</sub> levels for 24 hours and then subjected to (a) chemotaxis assay or (b) lysates were prepared and westerns performed to measure HIF-1 $\alpha$  levels with actin being used as a loading control. Shown is a representative blot. (c) Quantitation of relative HIF-1 $\alpha$  levels from three separate experiments. Additionally, Ramos B cells, stably transfected with lentiviral vectors over-expressing HIF-1 $\alpha$  (H), expressing firefly luciferase (C), or parental non-transfected Ramos cells (-), were incubated at the indicated O<sub>2</sub> levels for 24 hours and then subjected to (d) chemotaxis assay or (e) lysates were prepared and westerns performed to measure HIF-1 $\alpha$  levels with actin being used as a loading control. Shown is a representative blot. (f) Quantitation of relative HIF-1 $\alpha$  levels from three separate experiments. \*\*\* $P < 0.001$ ; \*\* $P < 0.01$

**Transient re-stabilization of HIF-1 $\alpha$  at 1% O<sub>2</sub> during CyA treatment partially restores CXCR4 hypo-responsiveness**

The above results demonstrated that CyA disrupts low O<sub>2</sub> dependent CXCR4 hypo-responsiveness in B cells, in part through HIF-1 $\alpha$  destabilization, and that DMOG

stabilization of HIF-1 $\alpha$  at 19% O<sub>2</sub> levels mimics the effects of low O<sub>2</sub>. We next asked whether transient DMOG addition at 1% O<sub>2</sub> levels during CyA treatment might, at least partially, restore O<sub>2</sub> dependent CXCR4 hypo-responsiveness. To test this hypothesis, we treated

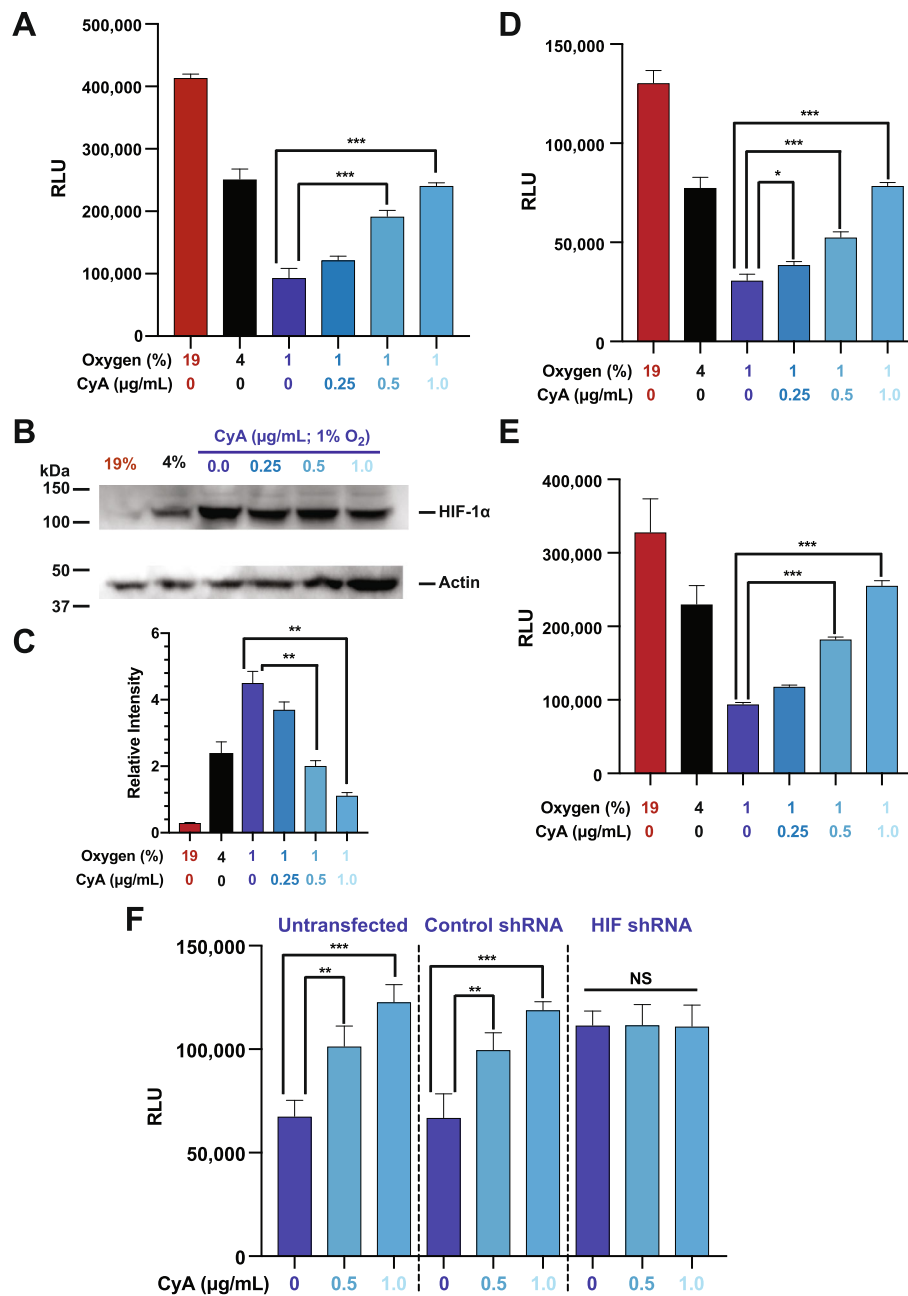


**Fig. 4** Cyclosporine A interferes with B cell hypoxia dependent CXCR4 hypo-responsiveness by destabilizing HIF-1α. Ramos cells were incubated at 19, 4 or 1% O<sub>2</sub> levels, with some 1% samples being incubated with the indicated concentrations CyA. After 24 hours the cells were subjected to (a) chemotaxis assay or (b) lysates were prepared and westerns performed to measure HIF-1α levels with actin being used as a loading control. Shown is a representative blot. (c) Quantitation of relative HIF-1α levels from three separate experiments. Primary human (d) or mouse (e) B cells were incubated at 19, 4 or 1% O<sub>2</sub> levels, with some 1% samples being incubated with the indicated concentrations CyA. After 24 hours a chemotaxis assay was performed. (f) Ramos B cells, stably transfected with lentiviral vectors expressing either HIF-1α shRNA (H), a scrambled non-specific control sequence shRNA (C) or parental non-transfected Ramos cells (-), were incubated at 1% O<sub>2</sub> levels with the indicated concentrations of CyA. After 24 hours the cells were subjected to the chemotaxis assay. \*\*\*P<0.001; \*\*P<0.01; \*P<0.05

RAMOS B cells with CyA for 24 hours, and during the last 3 or 6 hours of the incubation, DMOG was added. These experiments demonstrated that DMOG partially restored CXCR4 hypo-responsiveness of RAMOS cells, despite the presence of CyA (Fig. 5e).

**Proteomics reveals a group HIF-1α regulated proteins and their restoration by cyA**

To evaluate oxygen-dependent regulation of signaling components and their responsiveness to CyA, unbiased proteomics of RAMOS cell lysates at 19% and 1% O<sub>2</sub>

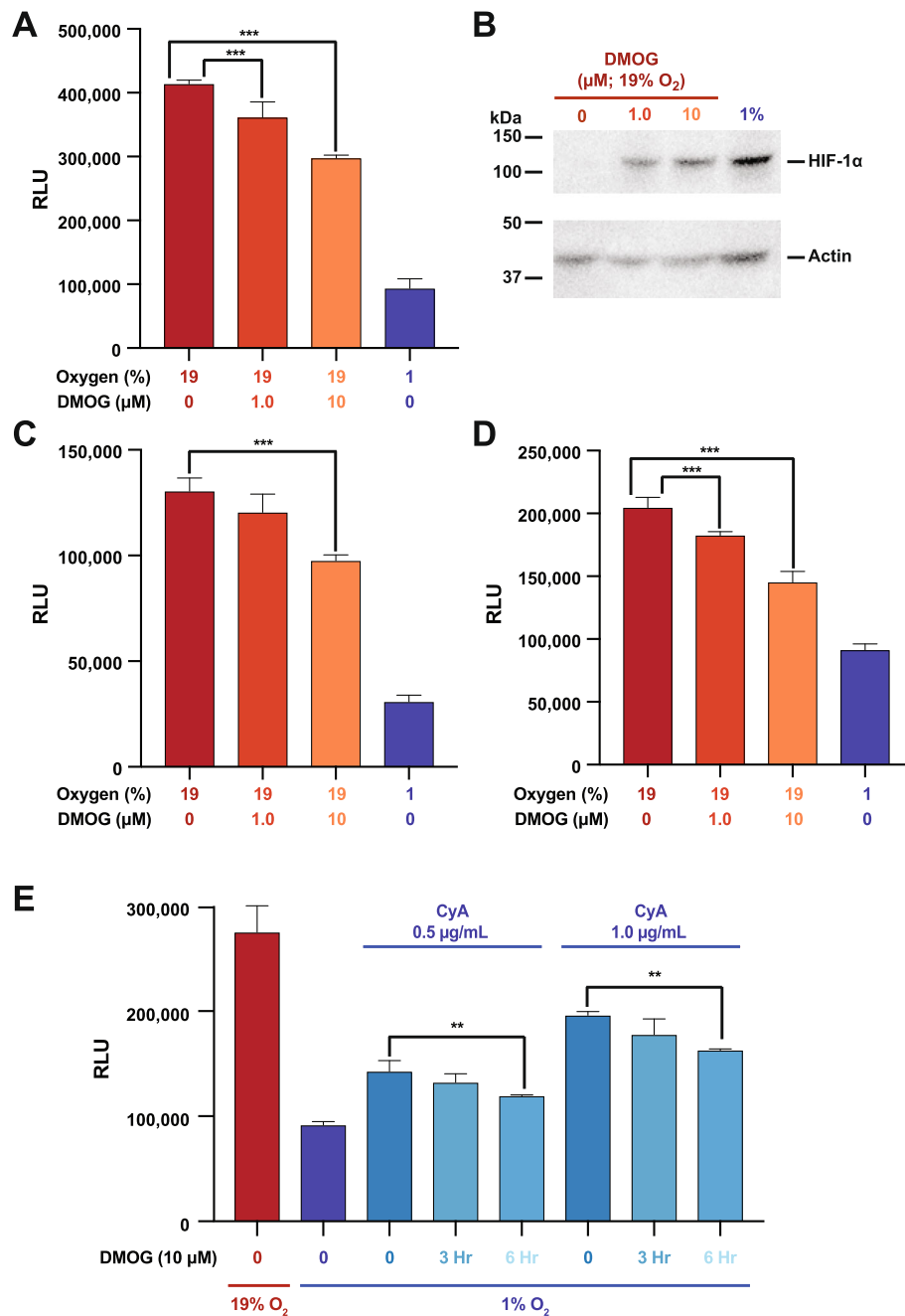


**Fig. 5** DMOG treatment of B cells stabilizes HIF-1 $\alpha$  and partially restores CXCR4 hypo-responsiveness in the presence of Cyclosporine A. RAMOS B cells (a), primary human peripheral blood B cells (c) or mouse splenic B cells (d) were incubated at 19% or 1%  $\text{O}_2$  levels for 24 hour with the indicated concentration of DMOG and then subjected to chemotaxis assay. (b) RAMOS cells lysates were assessed by western blot for HIF-1 $\alpha$  levels with actin being used as a loading control. Shown is a representative blot. (e) RAMOS B cells were incubated for 24 hours at either 19% or 1%  $\text{O}_2$  levels for 24 hours with the indicated concentration of CyA. Three or 6 hours before the end of the 24 hour incubation, DMOG was added to a final concentration of 10  $\mu\text{M}$  and then the cells were subjected to chemotaxis assay. \*\*\* $P < 0.001$ ; \*\* $P < 0.01$

levels, and at 1%  $\text{O}_2$  levels after CyA exposure was performed. Figure 6a shows 19 proteins that responded to the change in oxygen levels. Of these differentially expressed proteins, 7 had increased protein levels at 19%

$\text{O}_2$  and 12 were up-regulated under hypoxic conditions. These 12 up-regulated proteins included several regulated by HIF-1 $\alpha$  such as BCL2 Interacting Protein 3 (BNIP3), EGLN1 (Egl nine homolog 1), Protein FAM162A



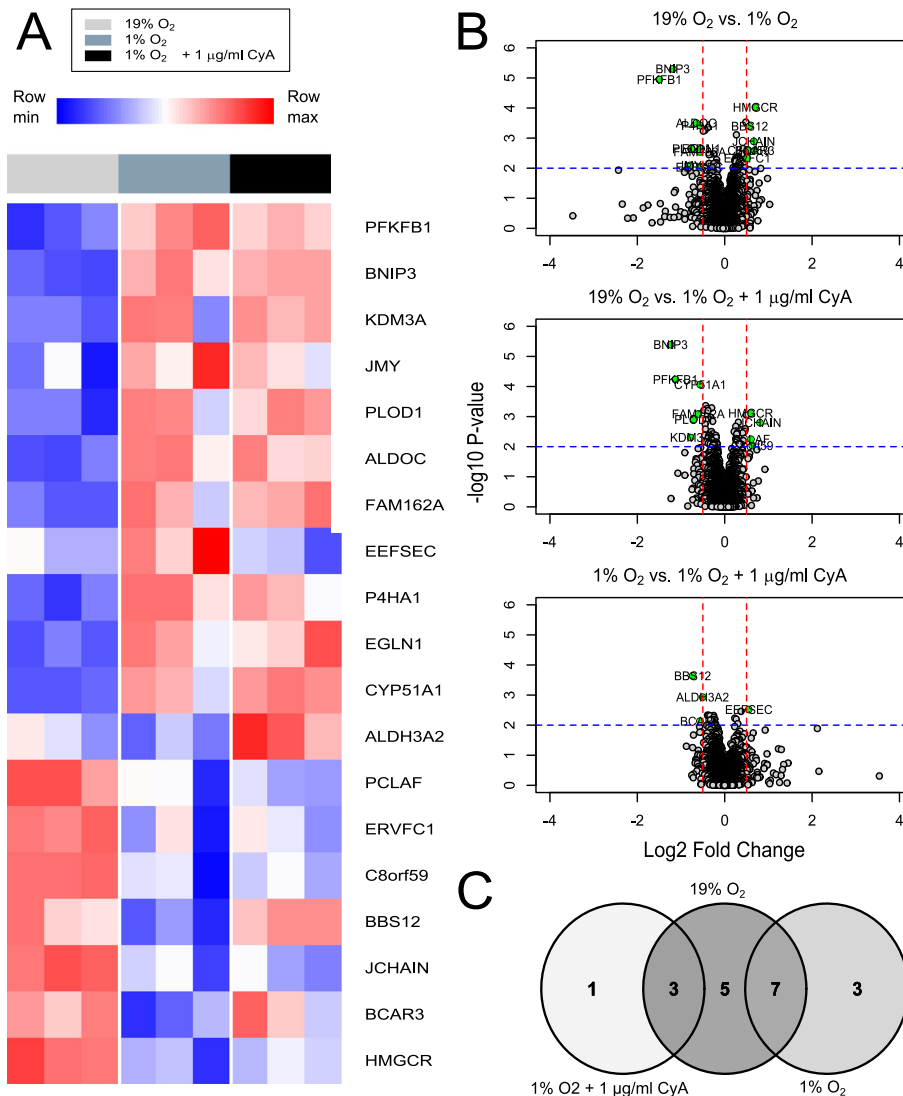


**Fig. 6** Differential expression analysis of proteomics data. **(a)** Heatmap of proteins with p-value  $\leq 0.01$  and  $\log_2FC \geq 0.5$  in any contrast. Color in each tile represents the scaled abundance value. **(b)** Volcano plots of proteins in the contrasts 19% O<sub>2</sub> vs. 1% O<sub>2</sub>, 19% O<sub>2</sub> vs. 1% O<sub>2</sub> + 1 µg/mL CyA, and 1% O<sub>2</sub> vs. 1% O<sub>2</sub> + 1 µg/mL CyA. **(c)** Venn diagram of proteins with differential abundances from the three contrasts

(FAM162A), Prolyl 4-hydroxylase subunit alpha-1 (P4HA1), Fructose-bisphosphate aldolase C (ALDOC), 6-phosphofructo-2-kinase/fructose-2,6-bisphosphatase (PFKFB1) and Procollagen-lysine,2-oxoglutarate 5-dioxygenase 1 (PLOD1). PLOD1 is a lysyl hydroxylase regulates extracellular matrix stiffening and collagen fiber alignment along with prolyl 4-hydroxylase subunit alpha-1 P4HA1 and HIF-1 $\alpha$  [40]. FAM162A [41] and BNIP3 [42] promote intrinsic apoptosis and autophagy in response to hypoxia via interactions with HIF-1 $\alpha$ .

Moreover, HIF-1 $\alpha$  coordinately represses and activates genes such as ALDOC and PFKFB1 to effect metabolic switching to a glycolytic state, providing biosynthetic substrates that facilitate proliferation [43].

We were particularly interested in proteins that were restored after treatment with CyA at 1% oxygen. The treatment with CyA restored the abundance of 3 proteins at 1% oxygen to a level similar to that in cells grown at 19% oxygen, selenocysteine-specific elongation factor (EEFSEC), Bardet-Biedl syndrome 12 protein (BBS12) and

breast cancer anti-estrogen resistance protein 3 (BCAR3). EEFSEC, BBS12 and BCAR3 have been shown to be responsive to cellular oxygen metabolism [44–46]. Pathway analysis of proteins differentially expressed with respect to 19% oxygen level were mapped to 21 pathways including HIF-1 $\alpha$  and glucose metabolism (Supplementary File 1). The two genes BNIP3 and EGLN1 involved in the HIF-1 $\alpha$  transcription factor pathway were only differentially expressed in the absence of CyA. Moreover, the CyA-modulated gene ALDH3A2 which is involved in many metabolic pathways including fatty acid and amino acid metabolism. Thus differential analysis revealed several signaling components that could be dysregulated in RAMOS cells due to hypoxia and further controlled by CyA.

#### Protein association networks identify signaling components perturbed by CyA

Differential analysis identified only 0.4% proteins to be responsive to the oxygen levels and/or CyA. To expand the search for relevant proteins we sought to investigate functionally related proteins both from (a) our dataset and (b) in the literature. We constructed a co-expression network in which high degree nodes are involved in several metabolic processes (Fig. 7a and Supplementary File 2 contains an edge list representation of the coexpression network). For example N6-adenosine-methyltransferase non-catalytic subunit (METTL14) is required in hypoxic stabilization of mRNAs [47] This is consistent with the known role of HIF-1 $\alpha$  in regulating metabolic switches.

We next compared the protein co-expression network with a knowledge-based network constructed using the STRING database [48] (Supplementary File 3). 72 nodes were present in both, the knowledge-based and co-expression networks. The top 20 proteins, sorted by node degree, and overlaid on a histogram of the degree distribution of the co-expression network highlights high-degree nodes from the two networks (Fig. 7a). Several overlapping high-degree nodes such as core-binding factor subunit beta (CBFB), clathrin light chain B (CLTB), phosphatidylinositol 4,5-bisphosphate 3-kinase catalytic subunit gamma isoform (PIK3CG) suggest their key role in the regulation of HIF-1 $\alpha$  and CyA signaling. Core-binding factor subunit beta is a master-regulator of genes involved in hematopoiesis (e.g., RUNX1) and osteogenesis (e.g., RUNX2). Clathrin light chain B is involved in receptor-mediated endocytosis [49].

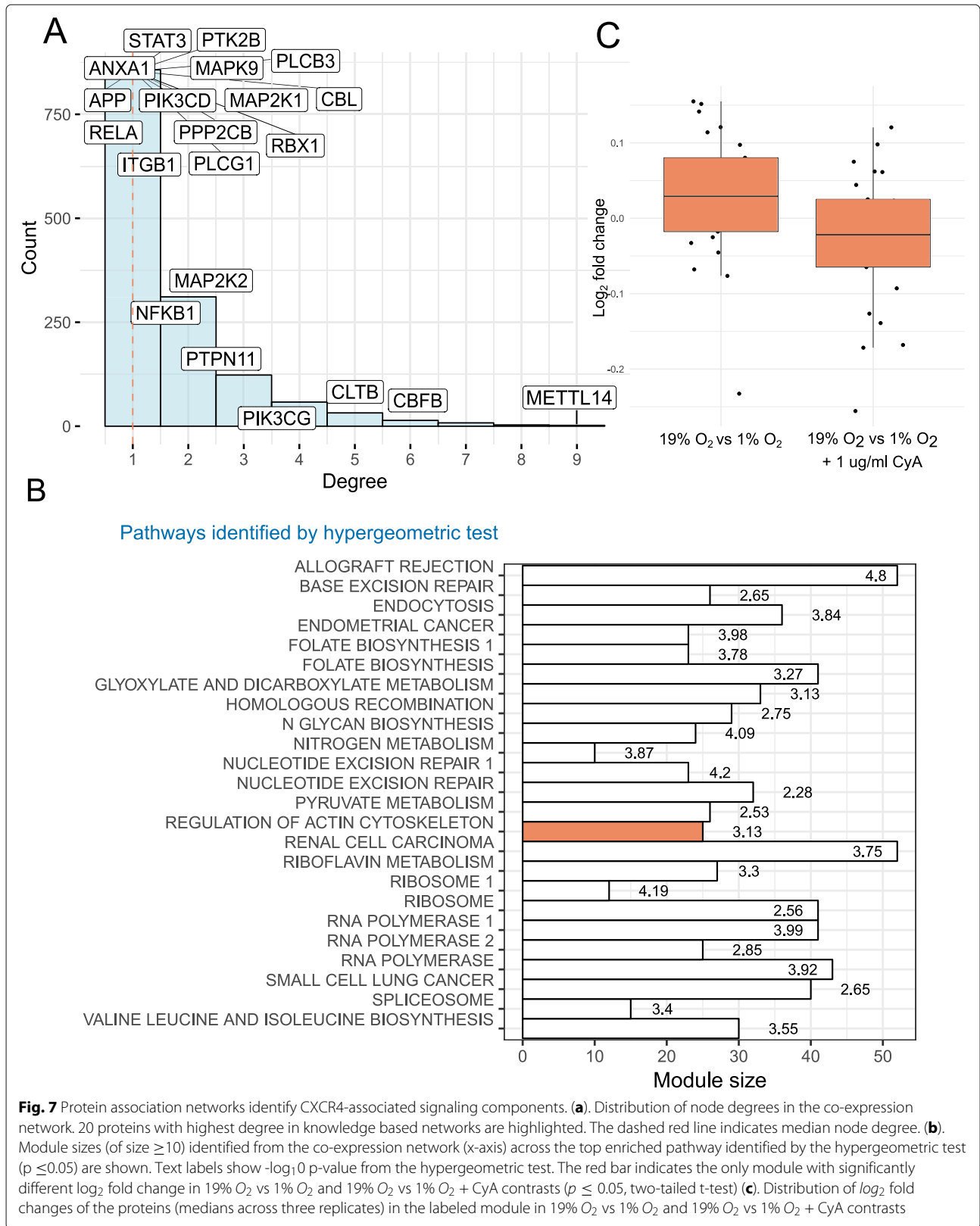
To identify modules of highly associated proteins, and by inference their genes, we used the edge-betweenness community detection algorithm [50]. We identified 24 communities with  $\geq 10$  proteins. These modules were characterized by the significantly enriched pathways (Fig. 7b). One community was of particular interest since it was restored after treatment with CyA at 1% O<sub>2</sub> (Fig. 7c)

and was enriched for proteins involved in regulation of the actin cytoskeleton (see Supplementary File 4 for a list of the top 3 enriched pathways, with associated p-values from the hypergeometric test). Specifically, this module contains the proteins PFN2 (profilin 2), IQGAP2 (Ras GTPase-like activating protein), and ITGAL (integrin alpha L). Both PFN2 [51] and IQGAP2 [52] regulate cell motility in response to intracellular signals. PFN2 is an epigenetic regulator of SMAD2/3 (Mothers against decapentaplegic homolog 2/3) [53], which in turn has been shown to promote metastasis in cancer cells [54]. SMAD2 and SMAD3 are also regulated by HIF-1 $\alpha$  [55]. In the knowledge-based STRING network, SMAD3 is directly linked to HIF-1 $\alpha$ . ITGAL is a target of the immunosuppressant drug efalizumab, which acts by reducing lymphocyte migration to sites of inflammation [56]. Thus, these proteins may be involved in the restoration of B cell chemotactic activity under hypoxic conditions by CyA, as measured by our chemotaxis assay, and suggest targets for further investigation.

#### Discussion

In this report we provide strong evidence for an O<sub>2</sub> sensing-HIF-1 $\alpha$  dependent molecular switch that alters human and mouse B cell chemokine receptor (CXCR4 and CXCR5) responsiveness, and that this switch is disrupted by the calcineurin inhibitor cyclosporine A (CyA). These results have broad implications for our understanding of normal B cell immunological processes. Critically, these effects occur naturally at differing O<sub>2</sub> levels in vivo in B cells, an aspect of immunological function that is often overlooked, and the particular importance of O<sub>2</sub> levels in B cell specific responses has only recently begun to come to light. In support of this view, recent work has shown that GC hypoxia itself is important for efficient B cell class switching, plasma cell differentiation and abundant antibody production [17]. In addition, hypoxia within the GC light zone has been reported to be critical for generation of high quality antibody responses, in part by creating a more stringent threshold for vital survival signals, leading to the selection and survival of B cell clones producing higher affinity immunoglobulin [57]. CXCR4 signaling has also been shown to be critical for normal B cell function and development [30, 32], especially proper B cell migration to, and localization within, the GC light or dark zones [58], and is dependent on CXCR4 signaling [28]. Increasingly hypoxia has been connected to CXCR4 regulation and function [33, 34]. Importantly, GC B cells reside within a highly hypoxic environment, express surface CXCR4, but are unresponsive to CXCL12 [34]. Thus, these reports support our experimental findings.

Combined, our results and previous reports link proper B cell GC localization through O<sub>2</sub> dependent differential CXCR4 responsiveness to optimum B cell responses. In



direct support of this hypothesis, we have found a HIF-1 $\alpha$  dependent O<sub>2</sub> sensing molecular switch that controls the responsiveness of CXCR4 to CXCL12, independent of CXCR4 surface expression, directly linking GC hypoxic conditions to CXCR4 signaling. Importantly, we show that CXCR4 responsiveness is modulated through O<sub>2</sub> levels that are physiological and observed within the LN in vivo. In particular, LN O<sub>2</sub> levels vary from 4-5% O<sub>2</sub> near afferent vessels to <1% in portions of the GC [17, 18, 34, 59]. Thus, it is very likely that this process is naturally coordinated and necessary for appropriate nodal and GC B cell dark/light zone localization, and that any disruption to this process would likely result in substandard B cell responses.

In addition to our functional findings, proteomics analysis identified signaling components involved in CXCR4 and HIF-1 $\alpha$  signaling that are modulated by CyA. The differential expression analysis also identified signaling pathways responding to hypoxia and their key regulators. Several of these pathways are associated with HIF-1 $\alpha$ , in agreement with findings of other groups [60–63]. However, several of the proteins reversing the effect of hypoxia with drug had lower fold-changes upon treatment with CyA. Association network analysis allowed us to probe CXCR4 and HIF-1 $\alpha$  signaling specifically even when CXCR4 expression itself was not changed. This analysis revealed key regulators involved in the response to CyA and hypoxia. Moreover, we identified a module that reversed the effect of hypoxia upon CyA treatment, as well as a novel, highly intra-correlated protein module potentially involved in the responsiveness to CyA. Further work will be needed to assess the dynamics of this protein network.

Our findings suggest a non-T cell dependent mechanism for calcineurin inhibitor (CNI) induced hypogammaglobulinemia and B cell hypo-responsiveness. CNI are commonly utilized to prevent allograft rejection in solid organ transplant recipients.[37-39] However, the overall immunosuppressive effects of CNI results in decreased antibody production and hypogammaglobulinemia. This can lead to greater morbidity and mortality associated with common infectious agents, such as influenza viruses [64–66]. Vaccination is generally recommended for transplant recipients, however, CNI-based immunosuppression also suppresses vaccine responses [2, 3]. This effect is largely thought to be due to CNI dependent inhibition of NFAT in helper T cells, leading to decreased T cell proliferation and IL-2 production [4]. Direct CNI effects on B cells have remained largely unidentified. However, we have now demonstrated that CyA has a novel and direct effect on B cell migration by disrupting the natural O<sub>2</sub> sensing molecular switch, destabilizing HIF-1 $\alpha$ , and allowing B cells to preserve CXCR4 responsiveness at low (<1%) O<sub>2</sub> levels. Preservation of CXCR4 responsiveness

disrupts coordinated GC B cell dark zone vs. light zone localization, which would suppress B cell responses in vivo. This is the first time, to our knowledge, that CyA have been shown to directly affect B cell migration, identifying a novel, and targetable, pathway by which CyA may directly affect B cell responses.

Improvement of immune function in CyA treated transplant patients during vaccination has the potential to increase vaccine efficacy, resulting in decreased morbidity and mortality associated with infection. However, as immune suppression is required to avoid allograft rejection, such immunological improvement would have to be transient and applied only during vaccine immune responses. We have identified a potential pathway to target, namely, reversal of CyA effects by transiently re-stabilizing HIF-1 $\alpha$ . Indeed our in vitro data demonstrates that transient re-stabilization of HIF-1 $\alpha$  through treatment of CyA affected B cells with the prolyl-4-hydroxylase (PHD) inhibitor dimethylallyl glycine (DMOG) results in retention of O<sub>2</sub> dependent changes in CXCR4 responsiveness. It is important to note that PHD inhibitors are clinically available for study, including FG-4592 and GSK1278863. Further pre-clinical study in mouse models would be required prior to clinical trials. Our data clearly demonstrate that both changes on O<sub>2</sub> levels and CyA levels identically affect the migratory capacity of mouse B and human B cells, strongly suggesting that direct in vivo data would be highly applicable to designing pre-clinical studies.

## Conclusions

We have characterized an O<sub>2</sub> sensing-HIF-1 $\alpha$  dependent molecular switch that alters human and mouse B cell CXCR4 responsiveness. This switch likely plays a significant role in GC B cell development and function. We have also identified a novel and direct CyA B cell affect whereby CyA directly interferes with this molecular switch by destabilizing HIF-1 $\alpha$  at low (<1%) O<sub>2</sub> levels, preserving both human and mouse B cell CXCR4 responsiveness. The clinical implications of these results are potentially profound, as they identify a readily targetable pathway, through the transient use of clinically available PHD inhibitors (e.g. FG-4592 and GSK1278863), which may improve vaccine responses in vulnerable immune suppressed transplant patients.

## Methods

### Human subjects protection

This study was approved by the Research Subjects Review Board at the University of Rochester Medical Center (RSRB #71460). Informed consent was obtained from all participants. Research data were coded such that subjects could not be identified, directly or through linked identifiers, in compliance with the Department of Health and

Human Services Regulations for the Protection of Human Subjects (45 CFR 46.101(b)(4)).

#### Human cell lines and primary b cell isolation

Human cell line: RAMOS (ATCC, Manassas, VA; CRL-1596) Burkitt's lymphoma B cell line was maintained in complete RPMI 1640 media supplemented with 10% FBS (cR10; Invitrogen, Carlsbad, CA). Primary human B cells: Human peripheral blood was collected by routine phlebotomy in heparinized vacutainers (BD Biosciences, San Diego, CA) and diluted 1:2 with PBS containing 2% FBS. Diluted blood was then layered over Ficoll-Paque PLUS (GE Healthcare, Chicago, IL) for density centrifugation using Sepmate tubes (Stemcell Technologies, Vancouver, BC, Canada). The lymphocyte layer was then washed twice with PBS (Invitrogen, Carlsbad, CA). PBMCs were then enriched for B cells by using the EasySep Human Pan-B cell Enrichment Kit (Stemcell Technologies, Vancouver, BC, Canada). PBMCs were incubated with an antibody cocktail containing CD2, CD3, CD14, CD16, CD36, Cd42b, CD56, CD66b, CD123, glycophorin A and dextran for 10 minutes. Streptavidin magnetic beads were added to the mix and the sample subjected to magnetic separation. The untouched enriched B cells were transferred to a clean tube, washed twice with PBS. B cells were then analyzed by flow cytometry showing >95% purity of the isolates.

#### Mouse splenic B cell isolation

Spleens from euthanized (carbon dioxide inhalation followed by exsanguination after severing the axillary artery and thoracotomy to ensure cessation of respiration and cardiac function) female 9-10 week old C57/Bl6 mice (Taconic Labs, Rensselaer, NY) were removed, mechanically dissociated and cell suspensions passed over a 100- $\mu$ m nylon cell strainer (BD Biosciences, San Diego, CA). Tissue remaining in the strainer was gently disrupted with the plunger of a 1 mL syringe, and the strainer rinsed with 5 mL of IMDM media (Invitrogen, Carlsbad, CA) containing 200 mM EDTA. The single cell suspension (SCS) was then passed over a 70- $\mu$ m nylon cell strainer (BD Biosciences, San Diego, CA) to further remove clumps. Excess RBCs were removed by magnetic positive selection (Imag; BD Biosciences, San Diego, CA) after incubation of the cell suspension with 50  $\mu$ L Ter119 magnetic beads (BD Biosciences, San Diego, CA) per  $1 \times 10^7$  total cells at 4°C for 30 min. Unbound cells were transferred to new tubes and washed once with PBS with 2% FBS and 0.4% EDTA. B cells were enriched from the SCS using Mouse Pan-B Cell Isolation kits (Stemcell Technologies, Vancouver, BC, Canada). Briefly, cells were suspended at  $1 \times 10^8$  cells/mL in PBS with 2% FBS and 0.4% EDTA. Normal Mouse serum was added at 50  $\mu$ L/mL followed by the Mouse Pan-B cell Isolation

Cocktail at 50  $\mu$ L/mL. Cells were incubated for 10 minutes at RT. RapidSpheres, at 50  $\mu$ L/mL, were added and incubated for 5 min. at RT. Samples were resuspended to a volume 2.5 mL with PBS with 2% FBS and 0.4% EDTA and placed on an Imag (BD Biosciences, San Diego, CA) for 5 min. Unbound cells were transferred to new tubes; flow cytometry indicated >95% purity of the isolates.

All research involving live, vertebrate animals was conducted in accordance with the Public Health Service Policy on Human Care and Use of Laboratory Animals. Female C57/Bl6 mice were obtained from Taconic Labs (Taconic Labs, Rensselaer, NY) and mice were maintained at the University of Rochester Medical Center Vivarium, an AAALAC certified Vivarium (Animal Welfare Assurance Number is A-3292-01), under their established guidelines, including isolation, feeding, recovery procedures, and euthanasia in accordance with Federal regulations. All experimental procedures for animals were approved by the Institutional Animal Care and Use Committee (IUCAC; protocol number UCAR-2011-055E), and all personnel working with the animals were trained and certified by the IUCAC and Vivarium staff.

#### Generation of stable HIF-1 $\alpha$ shRNA and HIF-1 $\alpha$ over-expression RAMOS cell lines

Lentiviral particles containing with HIF-1 $\alpha$  shRNA or a control shRNA encoding a scrambled shRNA sequence that will not lead to the specific degradation of any cellular message; or HIF-1 $\alpha$  activation particles or control particles expressing firefly luciferase, were obtained commercially (Santa Cruz Biotechnology, Dallas, TX). Stable transfectants were generated and selected using either puromycin (shRNA constructs) or blasticidin S (over-expression constructs) according to the manufacturer's recommendations (Santa Cruz Biotechnology, Dallas, TX).

#### O<sub>2</sub> controlled cell treatments

RAMOS B cells or human and mouse primary B cells were resuspended in cR10 media at  $5 \times 10^4$  cell/mL and added to appropriate sized tissue culture plates or flasks depending on total volume. To select flasks, CyA and/or DMOG (Sigma-Aldrich, St. Louis, MO) was added at the concentration indicated in the text and/or figure legends. Plates or flasks were then placed within controlled environment C-chamber 37°C, 5% CO<sub>2</sub> incubator inserts (Biospherix, Parish, NY) that were equilibrated O/N at the indicated O<sub>2</sub> levels or placed within a traditional 5% CO<sub>2</sub>, 37°C incubator (19% O<sub>2</sub>). Cells were incubated for 24 hours, removed and subjected to either the chemotaxis, western blot or proteomics assays.

### Chemotaxis assay

The human B cell line, RAMOS cells, or magnetic bead enriched primary human peripheral blood or mouse splenic B cells were resuspended in freshly prepared migration media (PBS + 1% BSA), and  $5 \times 10^5$  cells (in 75  $\mu\text{L}$ ) loaded into the upper chambers of 5  $\mu\text{m}$  polycarbonate 96 well transwell plates (Corning, Corning, NY). In triplicate wells, migration media containing varying concentrations of CXCL12 or CXCL13 was added to the bottom chambers of the transwells (225  $\mu\text{L}$  per well). Plates were incubated for 1 hour at appropriate  $\text{O}_2$  levels in the C-chamber incubator inserts (Biospherix, Parish, NY), at 37°C and 5%  $\text{CO}_2$ . Upper transwells were removed and 100  $\mu\text{L}$  of Cell Titer Glo (Promega, Madison, WI) added to each bottom well and incubated at RT for 10 min. Luminescence was readout on a Synergy™ HT microplate reader (BioTek Instruments, Winooski, VT) and relative luminescent units (RLU) reported. Supplementary Figure 4 demonstrates the direct correlation between RLU and cell numbers, through a  $4\text{-log}_{10}$  range, independent of  $\text{O}_2$  levels.

### Western blot

Nuclear lysates were prepared from B cell pellets using NE-PER nuclear and cytoplasmic extraction kits and protein concentration determined using micro BCA protein assay kits, both according to the manufacturer's recommendations (Thermo Fisher Scientific, Waltham, MA). Nuclear lysates (10  $\mu\text{g}$  per lane) were resolved on pre-cast NuPAGE 4-12% Bis-Tris protein gels (Invitrogen, Carlsbad, CA) and proteins transferred to PVDF membranes (Bio-Rad, Hercules, CA). The membrane was then blocked with 1X TBS-T (Tris-Buffered Saline (Bio-Rad, Hercules, CA)) with 0.05% Tween-20 (Sigma-Aldrich, St. Louis, MO) + 5% blotting grade non-fat dry milk (Bio-Rad, Hercules, CA) for 1 hour at RT. Blots were washed 3 x with TBS-T and then primary antibody diluted as indicated in TBS-T + 5% milk. For human B cell blots a 1:250 dilution mouse anti-human HIF-1 $\alpha$  (BD Biosciences, San Diego, CA) or for mouse blots a 1:100 dilution goat anti-mouse HIF-1 $\alpha$  was added and the blots incubated O/N at 4°C. As a loading control, blots were also probed with a 1:200 dilution mouse anti-actin primary antibody and the blots incubated O/N at 4°C. For detection of the human HIF-1 $\alpha$  or actin blots, a 1:1,000 dilution, in PBS + 5% milk, of horseradish peroxidase (HRP) conjugated goat anti-mouse Ig secondary was used. For mouse HIF-1 $\alpha$ , a 1:2,000 dilution HRP conjugated donkey anti-goat IgG was used. Secondaries were added and the blots incubated for 1 hour at RT. Blots were washed 3 X with TBS-T, rinsed with distilled water and freshly prepared ECL substrate (Thermo Fisher Scientific, Waltham, MA) added and the blots were imaged on a Chemi-Doc MP imaging system. Densitometry was performed

using Image Lab software version 6.0.1 (Bio-Rad, Hercules, CA).

### Proteomics

#### Sample preparation

RAMOS cells were re-suspended in cR10 media at  $5 \times 10^5$  cell/mL at a final volume of 10 mL in T25 tissue culture flasks (BD Biosciences, San Diego, CA) and either left untreated or cyclosporine A (Sigma-Aldrich, St. Louis, MO) added to a final concentration of 1  $\mu\text{g}/\text{mL}$ . Pairs of untreated or CyA treated cells were then incubated at either 19% or 1%  $\text{O}_2$  levels for 24 hours. Cells were then rapidly harvested into 50 mL conical tubes (BD Biosciences, San Diego, CA) containing 30 mL of ice cold PBS. Cells were pelleted and washed 3 x 10 mL ice cold PBS. After the final wash, cells were re-suspended in 1 mL ice cold PBS and transferred to a 1.5 mL microcentrifuge tubes and pelleted. Supernatants were removed and the cell pellets flash frozen in liquid nitrogen. Cell pellets were stored at  $-80^\circ\text{C}$  until samples were lysed for analysis.

Lysis buffer consisted of 5% SDS, 50 mM triethylammonium bicarbonate (TEAB). Cell lysis of each pellet was done by adding 100  $\mu\text{L}$  of lysis buffer per  $10^6$  cells, followed by vortexing and sonication using a QSonica sonicator. Sonication cycles consisted of 5 X 10 second sonications with one minute incubations on ice between each cycle. Samples were centrifuged for 5 minutes at 16,000 x g, and the supernatant was collected. Protein concentration was determined by BCA (Thermo Fisher Scientific, Waltham, MA). 25  $\mu\text{g}$  of protein from each sample was removed, and brought up to 25  $\mu\text{L}$  in lysis buffer. Disulfide bonds were reduced by addition of dithiothreitol (DTT) to 2 mM, followed by incubation at 55°C for 1 hour. Alkylation was performed by adding iodoacetamide to 10 mM and incubating at room temperature in the dark for 30 minutes. 12% phosphoric acid was added to a final concentration of 1.2%, followed by the addition of 6 volumes of 90% methanol, 100 mM TEAB. The resulting solution was added to S-Trap micros (Protifi, Huntington NY), and centrifuged at 4,000 x g for 1 minute. The S-Traps were washed twice with 90% methanol, 100 mM TEAB. 20  $\mu\text{L}$  of 100 mM TEAB containing 1  $\mu\text{g}$  of trypsin was added to the S-Trap, followed by an additional 20  $\mu\text{L}$  of TEAB.

Samples were placed in a humidity chamber at 37°C and were allowed to digest overnight. The S-Trap was centrifuged at 4,000 x g for 1 minute to collect the digested peptides. Twenty  $\mu\text{L}$  of 0.1% trifluoroacetic acid (TFA) in acetonitrile was added to the S-Trap, and one more centrifugation step was done, and the solutions were pooled, frozen, and dried down in a Speed Vac (Labconco, Kansas City, MO). Tandem mass tag (TMT) ten-plex reagents (0.2 mg) (Thermo Fisher Scientific, Waltham, MA) were removed from 20°C and allowed to reach room

temperature prior to dissolving each tag in 20  $\mu\text{L}$  of acetonitrile. Samples were re-constituted in 25  $\mu\text{L}$  of TEAB, the TMT tags were added to the samples, and incubated at room temperature for one hour. The reaction was quenched by the addition of 3  $\mu\text{L}$  of 5% hydroxylamine. 20% (5  $\mu\text{g}$ ) of each sample was combined, frozen, and dried in the Speed Vac.

To increase coverage, samples were fractionated using C18 spin columns. Columns were conditioned with acetonitrile, followed by equilibration with 100 mM ammonium formate (AF), pH 10. The samples were re-suspended in 50  $\mu\text{L}$  of AF and added to the spin columns. After washing the columns with water and then the AF buffer, samples were eluted with 10%, 12.5%, 15%, 17.5%, 20%, 22.5%, 25%, and then 50% acetonitrile in the AF buffer. These fractions were then frozen, dried down, and re-suspended in 0.1% TFA in water, and placed into autosampler vials.

#### Data acquisition

Peptides were injected onto a 30 cm C18 column packed with 1.8  $\mu\text{m}$  beads (Sepax), with an Easy nLC-1000 HPLC (Thermo Fisher Scientific, Waltham, MA), connected to a Q Exactive Plus mass spectrometer (Thermo Fisher Scientific, Waltham, MA). Solvent A was 0.1% formic acid in water, while solvent B was 0.1% formic acid in acetonitrile. Ions were introduced to the mass spectrometer using a Nanospray Flex source operating at 2 kV. The gradient began at 6% B and held for 2 minutes, increased to 30% B over 85 minutes, increased to 50% B over 10 minutes, then ramped up to 70% B in 4 minutes and was held for 5 minutes, before returning to starting conditions in 4 minutes and re-equilibrating for 10 minutes, for a total run time of 120 minutes at a 300 nL/minute flow rate. The Q Exactive Plus was operated in data-dependent mode, with a full scan followed by 10 MS/MS scans. The full scan was performed over a range of 400–1700 m/z, with a resolution of 70,000 at m/z of 200, an automatic gain control (AGC) target of  $10^6$ , and a maximum injection time of 50 ms. Peptides with a charge state between 2–5 were picked for fragmentation. Precursor ions were fragmented by higher-energy collisional dissociation (HCD) using a collision energy of 35 and an isolation width of 1.0 m/z. MS2 scans were collected with a resolution of 35,000, a maximum injection time of 120 ms, and an AGC setting of  $1e^5$ . The fixed first mass for the MS2 scans was set to 110 m/z to ensure TMT reporter ions were always collected. Dynamic exclusion was set to 25 seconds.

#### Data analysis

Raw data was searched using the SEQUEST search engine within the Proteome Discoverer software platform, version 2.2 (Thermo Fisher Scientific, Waltham, MA), using the SwissProt human database [67]. Trypsin was selected as the enzyme allowing up to 2 missed cleavages, with an

MS1 mass tolerance of 10 ppm, and an MS2 mass tolerance of 0.025 Da. Carbamidomethyl on cysteine, and TMT on lysine and peptide N-terminus were set as a fixed modifications, while oxidation of methionine was set as a variable modification. Percolator was used as the false discovery rate (FDR) calculator, filtering out peptides which had a q-value greater than 0.01. Reporter ions were quantified using the Reporter Ions Quantifier node, with an integration tolerance of 20 ppm, and the integration method being set to "most confident centroid". Protein abundances were calculated by summing the intensities of the reporter ions from each identified peptide, while excluding any peptides with an isolation interference of 30% or more. Low abundance proteins with less than one count per experiment/replicate were removed resulting in 5048 proteins. Proteins' abundance was  $\log_2$ -transformed, and normality was confirmed by diagnostic plots such as quantile-quantile plot. The differential expression analysis was performed using the implementation of the empirical Bayes statistic in the R package *limma* [68] across all conditions. Differentially expressed (DE) proteins are defined as p-value of  $\leq 0.01$  and a  $\log_2$ -fold change of  $\geq 0.5$ . Pathway analysis of DE proteins was performed using enricher from R package clusterProfiler [69] and 1392 canonical gene sets curated in MSigDB [70].

#### Network analysis

To evaluate the associations among proteins and neighborhood of DE proteins, we assembled a co-expression network using 3919 proteins with coefficient of variation  $\geq 0.01$  (Supplementary File 2). The edges were weighted by the absolute Pearson correlation coefficient between the connected nodes. Each edge in the co-expression network was assigned a z-score by permutation of sample labels 50 times. We retained only edges with a weight (Pearson correlation coefficient) that had an absolute z-score of  $\geq 1.5$ , i.e., the real correlation was at least 1.5 standard deviations away from the mean of correlations calculated by perturbing sample labels. Edges with a weight  $\leq 0.5$  were removed. This resulted in a network of 1408 nodes and 1211 edges. The implementation of the edge-betweenness community detection algorithm in the R package *igraph* [50, 71] was used to identify communities with  $\geq 10$  genes. We performed a gene set enrichment analysis using the hypergeometric test. To further map genes/proteins known to be functionally related to HIF1A and CXCR4, 33 pathways from KEGG [72], Biocarta [73] and Reactome [74] were identified. The compiled list of 1504 unique genes from these pathways was used in the STRING database [48] to build a network where the edges are weighted based on strength of experimental evidence of interaction, co-expression measured using data in public domain, and database annotations. This network is referred to as the *knowledge based network*.

The complete list of interactions is provided in the Supplementary File 3.

### Statistics

Permutation tests within the general linear models framework were used to fit the data to compare differences groups. Group comparisons of interest were obtained by pairwise comparisons using Tukey's method to control for the multiple testing error rate. We adjusted for CXCL12 concentrations in the models when HIF-1 $\alpha$  levels were compared across multiple CXCL12 concentrations. The statistical analyses were conducted using the *lmPerm* and *multcomp* packages within the statistical analysis software R version 3.5.1 [75, 76]. The significance level for all tests was set at 5%.

### Supplementary information

**Supplementary information** accompanies this paper at <https://doi.org/10.1186/s12865-020-0342-8>.

**Additional file 1:** Supplementary figures.

**Additional file 2:** Results of Pathway Analysis. Data provided as an Excel spread sheet.

**Additional file 3:** Coexpression Network. Data provided as a txt file.

**Additional file 4:** Curated Network. Data provided as an Excel spread sheet.

**Additional file 5:** Top 3 enriched pathways, with associated p-values from the hypergeometric test. Data provided as an Excel spread sheet.

### Abbreviations

AF: ammonium formate; AGC: automatic gain control; BCA: bicinchoninic acid; CD: cluster of differentiation; CNl: Calcineurin inhibitors; CyA: cyclosporine A; DMOG: dimethylloxallyl glycine; DTT: dithiothreitol; ECL: enhanced chemiluminescence; EDTA: ethylenediaminetetraacetic acid; FAK: Focal adhesion kinase; FBS: fetal bovine serum; FDR: false discovery rate; GC: Germinal center; HCD: higher-energy collisional dissociation; HIF: Hypoxia inducible factor; HPLC: high performance liquid chromatography; HRP: horseradish peroxidase; IL-2: Interleukin 2; IMDM: Iscove's modified Dulbecco's medium; LN: Lymph node; MAPK: Mitogen-activated protein kinase; MKP-1: MAP kinase phosphatase 1; NFAT: Nuclear factor of activated T-cells; O/N: Overnight; PBMC: peripheral blood mononuclear cell; PBS: phosphate-buffered saline; PHD: prolyl-4-hydroxylase; PVDF: polyvinylidene difluoride; RBCs: Red blood cells; RGS1: Regulator Of G Protein Signaling 1; RLU: relative luminescent units; RPMI: Roswell Park Memorial Institute; RT: room temperature; SCS: single cell suspension; shRNA: Small hairpin ribonucleic acid; TBS-T: TBS with tween-20; TBS: tris-buffered saline; TEAB: triethylammonium bicarbonate; TFA: trifluoroacetic acid; TMT: tandem mass tag

### Acknowledgements

The authors would like to thank Alexander Wiltse for his excellent technical assistance, and critical reading of the manuscript. We would also like to thank Dr. Alicia Henn and the other members of Biospherix for their assistance setting up and providing recommendations for operating the O<sub>2</sub> controlled CO<sub>2</sub> incubator inserts.

### Authors' contributions

SPH conceived of the research, performed research, and wrote the manuscript. MGP performed a portion of the analysis, and wrote the manuscript. JAE performed research. DL performed a portion of the analysis, and wrote the manuscript. JG performed the research. JW performed research. ESM performed research. VC performed research. JT conceived of the proteomics analysis, and wrote the manuscript. MSZ conceived of the research, and wrote the manuscript. All authors have read and approved the manuscript.

### Funding

This work was supported by grants from the National Institutes of Health, National Institutes of Allergy and Infectious Diseases, including: AI134058 (SPH, MSZ, MGP, JT, JAE, ESM, JG, VC), AI098112, and AI069351 (MSZ, SPH, JG, JW), P30AI078498 (MSZ), as well as the University of Rochester Clinical and Translational Science Award UL1 TR002001 from the National Center for Advancing Translational Sciences of the National Institutes of Health (DL, MZ). The content is solely the responsibility of the authors and does not necessarily represent the official views of the National Institutes of Health. None of the above funders had any role in study design, data collection and analysis, decision to publish, or preparation of the manuscript.

### Availability of data and materials

Data are included in Supplemental Files. The remainder of the reagents are available publicly, as referenced in the "Methods" section.

### Ethics approval and consent to participate

This study was approved by the Research Subjects Review Board at the University of Rochester Medical Center. (RSRB Protocol 71460), and all subjects gave written informed consent as described in the "Methods" section above.

### Consent for publication

Not applicable.

### Competing interests

The authors declare that they have no competing interests.

### Author details

<sup>1</sup>University of Rochester Medical Center, Division of Nephrology, 601 Elmwood Ave., 14642 Rochester, NY, USA. <sup>2</sup>University of Rochester, Biophysics, Structural, and Computational Biology Program, 601 Elmwood Ave. - Box 675, 14642 Rochester, NY, USA. <sup>3</sup>University of Rochester, Clinical and Translational Science Institute, 265 Crittenden Blvd., 14642 Rochester, NY, USA. <sup>4</sup>University of Rochester, Department of Microbiology and Immunology, 601 Elmwood Ave - Box 672, 14642 Rochester, NY, USA. <sup>5</sup>University of Rochester, Department of Biostatistics and Computational Biology, 265 Crittenden Blvd., 14642 Rochester, NY, USA.

Received: 2 May 2019 Accepted: 27 February 2020

Published online: 18 March 2020

### References

- Malat G, Culkin C. The abcs of immunosuppression: A primer for primary care physicians. *Med Clin North Am.* 2016;100(3):505–18. <https://doi.org/10.1016/j.mcna.2016.01.003>.
- Felldin M, Andersson B, Studahl M, Svennerholm B, Friman V. Antibody persistence 1 year after pandemic h1n1 2009 influenza vaccination and immunogenicity of subsequent seasonal influenza vaccine among adult organ transplant patients. *Transpl Int.* 2014;27(2):197–203. <https://doi.org/10.1111/tri.12237>.
- Felldin M, Studahl M, Svennerholm B, Friman V. The antibody response to pandemic h1n1 2009 influenza vaccine in adult organ transplant patients. *Transpl Int.* 2012;25(2):166–71. <https://doi.org/10.1111/j.1432-2277.2011.01391.x>.
- Heidt S, Roelen DL, Eijnsink C, Eikmans M, van Kooten C, Claas FH, Mulder A. Calcineurin inhibitors affect b cell antibody responses indirectly by interfering with t cell help. *Clin Exp Immunol.* 2010;159(2):199–207. <https://doi.org/10.1111/j.1365-2249.2009.04051.x>.
- KIM H-S, RASKOVA J, DEGIANNIS D, RASKA JR K. Effects of cyclosporine and rapamycin on immunoglobulin production by preactivated human b cells. *Clin Exp Immunol.* 1994;96(3):508–12. <https://doi.org/10.1111/j.1365-2249.1994.tb06058.x>.
- Palazon A, Goldrath AW, Nizet V, Johnson RS. Hif transcription factors, inflammation, and immunity. *Immunity.* 2014;41(4):518–28. <https://doi.org/10.1016/j.immuni.2014.09.008>.
- Cramer T, Yamanishi Y, Clausen BE, Forster I, Pawlinski R, Mackman N, Haase VH, Jaenisch R, Corr M, Nizet V, Firestein GS, Gerber HP, Ferrara N, Johnson RS. Hif-1alpha is essential for myeloid cell-mediated inflammation. *Cell.* 2003;112(5):645–57.
- Dang EV, Barbi J, Yang HY, Jinasena D, Yu H, Zheng Y, Bordman Z, Fu J, Kim Y, Yen HR, Luo W, Zeller K, Shimoda L, Topalian SL, Sementza GL,



- Dang CV, Pardoll DM, Pan F. Control of t(h)17/t(reg) balance by hypoxia-inducible factor 1. *Cell*. 2011;146(5):772–84. <https://doi.org/10.1016/j.cell.2011.07.033>.
9. Doedens AL, Phan AT, Stradner MH, Fujimoto JK, Nguyen JV, Yang E, Johnson RS, Goldrath AW. Hypoxia-inducible factors enhance the effector responses of cd8(+) t cells to persistent antigen. *Nat Immunol*. 2013;14(11):1173–82. <https://doi.org/10.1038/ni.2714>.
  10. McNamee EN, Korn Johnson D, Homann D, Clambey ET. Hypoxia and hypoxia-inducible factors as regulators of t cell development, differentiation, and function. *Immunol Res*. 2013;55(1-3):58–70. <https://doi.org/10.1007/s12026-012-8349-8>.
  11. Walmsley SR, Print C, Farahi N, Peyssonnaud C, Johnson RS, Cramer T, Sobolewski A, Condliffe AM, Cowburn AS, Johnson N, Chilvers ER. Hypoxia-induced neutrophil survival is mediated by hif-1alpha-dependent nf-kappab activity. *J Exp Med*. 2005;201(1):105–15. <https://doi.org/10.1084/jem.20040624>.
  12. Liu S, Shah SJ, Wilmes LJ, Feiner J, Kodibagkar VD, Wendland MF, Mason RP, Hylton N, Hopf HW, Rollins MD. Quantitative tissue oxygen measurement in multiple organs using 19f mri in a rat model. *Magn Reson Med*. 2011;66(6):1722–30. <https://doi.org/10.1002/mrm.22968>.
  13. Carreau A, El Hafny-Rahbi B, Matejuk A, Grillon C, Kieda C. Why is the partial oxygen pressure of human tissues a crucial parameter? small molecules and hypoxia. *J Cell Mol Med*. 2011;15(6):1239–53. <https://doi.org/10.1111/j.1582-4934.2011.01258.x>.
  14. Caldwell CC, Kojima H, Lukashew D, Armstrong J, Farber M, Apasov SG, Sitkovsky MV. Differential effects of physiologically relevant hypoxic conditions on t lymphocyte development and effector functions. *J Immunol*. 2001;167(11):6140–9.
  15. Huang JH, Cardenas-Navia LI, Caldwell CC, Plumb TJ, Radu CG, Rocha PN, Wilder T, Bromberg JS, Cronstein BN, Sitkovsky M, Dewhirst MW, Dustin ML. Requirements for t lymphocyte migration in explanted lymph nodes. *J Immunol*. 2007;178(12):7747–55.
  16. Asosingh K, De Raeve H, de Ridder M, Storme GA, Willems A, Van Riet I, Van Camp B, Vanderkerken K. Role of the hypoxic bone marrow microenvironment in 5t2mm murine myeloma tumor progression. *Haematologica*. 2005;90(6):810–7.
  17. Abbott RK, Thayer M, Labuda J, Silva M, Philbrook P, Cain DW, Kojima H, Hatfield S, Sethumadhavan S, Ohta A, Reinherz EL, Kelseo G, Sitkovsky M. Germinal center hypoxia potentiates immunoglobulin class switch recombination. *J Immunol*. 2016;197(10):4014–20. <https://doi.org/10.4049/jimmunol.1601401>.
  18. Cho SH, Raybuck AL, Stengel K, Wei M, Beck TC, Volanakis E, Thomas JW, Hiebert S, Haase VH, Boothby MR. Germinal centre hypoxia and regulation of antibody qualities by a hypoxia response system. *Nature*. 2016;537(7619):234–8. <https://doi.org/10.1038/nature19334>.
  19. Ikejiri A, Nagai S, Goda N, Kurebayashi Y, Osada-Oka M, Takubo K, Suda T, Koyasu S. Dynamic regulation of th17 differentiation by oxygen concentrations. *Int Immunol*. 2012;24(3):137–46. <https://doi.org/10.1093/intimm/dxr111>.
  20. Makino Y, Nakamura H, Ikeda E, Ohnuma K, Yamauchi K, Yabe Y, Poellinger L, Okada Y, Morimoto C, Tanaka H. Hypoxia-inducible factor regulates survival of antigen receptor-driven t cells. *J Immunol*. 2003;171(12):6534–40.
  21. Nakamura H, Makino Y, Okamoto K, Poellinger L, Ohnuma K, Morimoto C, Tanaka H. Tcr engagement increases hypoxia-inducible factor-1 alpha protein synthesis via rapamycin-sensitive pathway under hypoxic conditions in human peripheral t cells. *J Immunol*. 2005;174(12):7592–9.
  22. Stewart M, Talks K, Leek R, Turley H, Pezzella F, Harris A, Gatter K. Expression of angiogenic factors and hypoxia inducible factors hif 1, hif 2 and ca ix in non-hodgkin's lymphoma. *Histopathology*. 2002;40(3):253–60.
  23. Evens AM, Schumacker PT, Helenowski IB, Singh AT, Dokic D, Keswani A, Kordeluk E, Raji A, Winter JN, Jovanovic BD, Holmgren A, Nelson BP, Gordon LI. Hypoxia inducible factor-alpha activation in lymphoma and relationship to the thioredoxin family. *Br J Haematol*. 2008;141(5):676–80. <https://doi.org/10.1111/j.1365-2141.2008.07093.x>.
  24. Evens AM, Sehn LH, Farinha P, Nelson BP, Raji A, Lu Y, Brakman A, Parimi V, Winter JN, Schumacker PT, Gascoyne RD, Gordon LI. Hypoxia-inducible factor-1 alpha expression predicts superior survival in patients with diffuse large b-cell lymphoma treated with r-chop. *J Clin Oncol*. 2010;28(6):1017–24. <https://doi.org/10.1200/JCO.2009.24.1893>.
  25. Henn AD, Laski M, Yang H, Welle S, Qiu X, Miao H, Barry CT, Wu H, Zand MS. Functionally distinct subpopulations of cpq-activated memory b cells. *Sci Rep*. 2012;2:345. <https://doi.org/10.1038/srep00345>.
  26. Henn AD, Wu S, Qiu X, Ruda M, Stover M, Yang H, Liu Z, Welle SL, Holden-Wiltse J, Wu H, Zand MS. High-resolution temporal response patterns to influenza vaccine reveal a distinct human plasma cell gene signature. *Sci Rep*. 2013;3:2327. <https://doi.org/10.1038/srep02327>.
  27. Shapiro-Shelef M, Calame K. Regulation of plasma-cell development. *Nat Rev Immunol*. 2005;5(3):230–42. <https://doi.org/10.1038/nri1572>.
  28. Allen CD, Ansel KM, Low C, Lesley R, Tamamura H, Fujii N, Cyster JG. Germinal center dark and light zone organization is mediated by cxcr4 and cxcr5. *Nat Immunol*. 2004;5(9):943–52. <https://doi.org/10.1038/ni1100>.
  29. Kabashima K, Haynes NM, Xu Y, Nutt SL, Allende ML, Proia RL, Cyster JG. Plasma cell s1p1 expression determines secondary lymphoid organ retention versus bone marrow tropism. *J Exp Med*. 2006;203(12):2683–90. <https://doi.org/10.1084/jem.20061289>.
  30. Nie Y, Waite J, Brewer F, Sunshine MJ, Littman DR, Zou YR. The role of cxcr4 in maintaining peripheral b cell compartments and humoral immunity. *J Exp Med*. 2004;200(9):1145–56. <https://doi.org/10.1084/jem.20041185>.
  31. Kehrl JH, Hwang IY, Park C. Chemoattractant receptor signaling and its role in lymphocyte motility and trafficking. *Curr Top Microbiol Immunol*. 2009;334:107–27. <https://doi.org/10.1007/978-3-540-93864-4-5>.
  32. Busillo JM, Benovic JL. Regulation of cxcr4 signaling. *Biochim Biophys Acta*. 2007;1768(4):952–63. <https://doi.org/10.1016/j.bbame.2006.11.002>.
  33. Schioppa T, Uranchimeg B, Saccani A, Biswas SK, Doni A, Rapisarda A, Bernasconi S, Saccani S, Nebuloni M, Vago L, Mantovani A, Melillo G, Sica A. Regulation of the chemokine receptor cxcr4 by hypoxia. *J Exp Med*. 2003;198(9):1391–402. <https://doi.org/10.1084/jem.20030267>.
  34. Piovani E, Tosello V, Indraccolo S, Masiero M, Persano L, Esposito G, Zamarchi R, Ponzoni M, Chieco-Bianchi L, Dalla-Favera R, Amadori A. Differential regulation of hypoxia-induced cxcr4 triggering during b-cell development and lymphomagenesis. *Cancer Res*. 2007;67(18):8605–14. <https://doi.org/10.1158/0008-5472.CAN-06-4722>.
  35. Corley KM, Taylor CJ, Lilly B. Hypoxia-inducible factor 1alpha modulates adhesion, migration, and fak phosphorylation in vascular smooth muscle cells. *J Cell Biochem*. 2005;96(5):971–85. <https://doi.org/10.1002/jcb.20559>.
  36. D'Angelo G, Duplan E, Vigne P, Frelin C. Cyclosporin a prevents the hypoxic adaptation by activating hypoxia-inducible factor-1alpha pro-564 hydroxylation. *J Biol Chem*. 2003;278(17):15406–11. <https://doi.org/10.1074/jbc.M211293200>.
  37. Vandyke K, Zeissig MN, Hewett DR, Martin SK, Mrozik KM, Cheong CM, Diamond P, To LB, Gronthos S, Peet DJ, Croucher PI, Zannettino ACW. Hif-2alpha promotes dissemination of plasma cells in multiple myeloma by regulating cxcl12/cxcr4 and ccr1. *Cancer Res*. 2017;77(20):5452–63. <https://doi.org/10.1158/0008-5472.CAN-17-0115>.
  38. Fujita N, Chiba K, Shapiro IM, Risbud MV. Hif-1alpha and hif-2alpha degradation is differentially regulated in nucleus pulposus cells of the intervertebral disc. *J Bone Miner Res*. 2012;27(2):401–12. <https://doi.org/10.1002/jbmr.538>.
  39. Kahan BD. Therapeutic drug monitoring of cyclosporine: 20 years of progress. *2 Suppl*. 2004;36:378–91. <https://doi.org/10.1016/j.transproceed.2004.01.091>.
  40. Gilkes DM, Bajpai S, Chaturvedi P, Wirtz D, Semenza GL. Hypoxia-inducible factor 1 (hif-1) promotes extracellular matrix remodeling under hypoxic conditions by inducing p4ha1, p4ha2, and plod2 expression in fibroblasts. *J Biol Chem*. 2013;288(15):10819–29. <https://doi.org/10.1074/jbc.M112.442939>.
  41. Kim J-Y, Kim S-M, Ko J-H, Yim J-H, Park J-H. Interaction of pro-apoptotic protein hgt-d-p with heat shock protein 90 is required for induction of mitochondrial apoptotic cascades. *2006;580(13):3270–3275*. <https://doi.org/10.1016/j.febslet.2006.05.001>.
  42. Bellot G, Garcia-Medina R, Gounon P, Chiche J, Roux D, Pouyssegur J, Mazure NM. Hypoxia-induced autophagy is mediated through hypoxia-inducible factor induction of bnip3 and bnip3l via their bh3 domains. *Mol Cell Biol*. 2009;29(10):2570–81. <https://doi.org/10.1128/MCB.00166-09>.
  43. Vander Heiden MG, Cantley LC, Thompson CB. Understanding the warburg effect: the metabolic requirements of cell proliferation. *Science*. 2009;324(5930):1029–33. <https://doi.org/10.1126/science.1160809>.
  44. Steimbrenner H, Sies H. Protection against reactive oxygen species by selenoproteins. *Biochim Biophys Acta*. 2009;1790(11):1478–85. <https://doi.org/10.1016/j.bbagen.2009.02.014>.

45. Sosa MS, Lopez-Haber C, Yang C, Wang H, Lemmon MA, Busillo JM, Luo J, Benovic JL, Klein-Szanto A, Yagi H, Gutkind JS, Parsons RE, Kazanietz MG. Identification of the rac-gef p-rex1 as an essential mediator of erbB signaling in breast cancer. *Molecular Cell*. 2010;40(6):877–92. <https://doi.org/10.1016/j.molcel.2010.11.029>.
46. Marion V, Mockel A, De Melo C, Obringer C, Claussmann A, Simon A, Messaddeq N, Durand M, Dupuis L, Loeffler J-P, King P, Mutter-Schmidt C, Petrovsky N, Stoetzel C, Dollfus H. Bbs-induced ciliary defect enhances adipogenesis, causing paradoxical higher-insulin sensitivity, glucose usage, and decreased inflammatory response. *Cell Metabol*. 2012;16(3):363–77. <https://doi.org/10.1016/j.cmet.2012.08.005>.
47. Fry NJ, Law BA, Ilkayeva OR, Holley CL, Mansfield KD. N(6)-methyladenosine is required for the hypoxic stabilization of specific mRNAs. *Rna*. 2017;23(9):1444–55. <https://doi.org/10.1261/rna.061044.117>.
48. Gable AL, Szklarczyk D, Lyon D, Simonovic M, Wyder S, Mering Cv, Junge A, Jensen LJ, Doncheva NT, Huerta-Cepas J, Morris JH, Bork P. STRING v11: protein–protein association networks with increased coverage, supporting functional discovery in genome-wide experimental datasets. *Nucleic Acids Res*. 2018;47(D1):607–13. <https://doi.org/10.1093/nar/gky1131>.
49. Incardona JP, Lee JH, Robertson CP, Enga K, Kapur RP, Roelink H. Receptor-mediated endocytosis of soluble and membrane-tethered sonic hedgehog by patched-1. *Proc Natl Acad Sci U S A*. 2000;97(22):12044–9. <https://doi.org/10.1073/pnas.220251997>.
50. Newman MEJ. Detecting community structure in networks. *Eur Phys J B*. 2004;38(2):321–30. <https://doi.org/10.1140/epjb/e2004-00124-y>.
51. Mouneimne G, Hansen SD, Selfors LM, Petrak L, Hickey MM, Gallegos LL, Simpson KJ, Lim J, Gertler FB, Hartwig JH, Mullins RD, Brugge JS. Differential remodeling of actin cytoskeleton architecture by profilin isoforms leads to distinct effects on cell migration and invasion. *Cancer Cell*. 2012;22(5):615–30. <https://doi.org/10.1016/j.ccr.2012.09.027>.
52. Hedman AC, Smith JM, Sacks DB. The biology of iqqap proteins: beyond the cytoskeleton. *EMBO Rep*. 2015;16(4):427–46. <https://doi.org/10.15252/embr.201439834>.
53. Kim MJ, Lee YS, Han GY, Lee HN, Ahn C, Kim CW. Profilin 2 promotes migration, invasion, and stemness of ht29 human colorectal cancer stem cells. *Biosci Biotechnol Biochem*. 2015;79(9):1438–46. <https://doi.org/10.1080/09168451.2015.1043118>.
54. Tang YN, Ding WQ, Guo XJ, Yuan XW, Wang DM, Song JG. Epigenetic regulation of smad2 and smad3 by profilin-2 promotes lung cancer growth and metastasis. *Nat Commun*. 2015;6:8230. <https://doi.org/10.1038/ncomms9230>.
55. Mingyuan X, Qianqian P, Shengquan X, Chenyi Y, Rui L, Yichen S, Jinghong X. Hypoxia-inducible factor-1 $\alpha$  activates transforming growth factor- $\beta$ 1/smad signaling and increases collagen deposition in dermal fibroblasts. *Oncotarget*. 2017;9(3):3188–97. <https://doi.org/10.18632/oncotarget.23225>.
56. Lebwohl M, Tying SK, Hamilton TK, Toth D, Glazer S, Tawfik NH, Walicke P, Dummer W, Wang X, Garovoy MR, Pariser D. A novel targeted t-cell modulator, efalizumab, for plaque psoriasis. *N Engl J Med*. 2003;349(21):2004–13. <https://doi.org/10.1056/NEJMoa030002>.
57. Pereira JP, Kelly LM, Cyster JG. Finding the right niche: B-cell migration in the early phases of t-dependent antibody responses. *Int Immunol*. 2010;22(6):413–9. <https://doi.org/10.1093/intimm/dxq047>.
58. Bannard O, Horton RM, Allen CD, An J, Nagasawa T, Cyster JG. Germinal center centroblasts transition to a centrocyte phenotype according to a timed program and depend on the dark zone for effective selection. *Immunity*. 2013;39(5):912–24. <https://doi.org/10.1016/j.immuni.2013.08.038>.
59. Zenewicz LA. Oxygen levels and immunological studies. *Front Immunol*. 2017;8:324. <https://doi.org/10.3389/fimmu.2017.00324>.
60. Gao P, Yang C, Nesvick CL, Feldman MJ, Sizzdahkhani S, Liu H, Chu H, Yang F, Tang L, Tian J, Zhao S, Li G, Heiss JD, Liu Y, Zhuang Z, Xu G. Hypotaurine evokes a malignant phenotype in glioma through aberrant hypoxic signaling. *Oncotarget*. 2016;7(12):15200–14. <https://doi.org/10.18632/oncotarget.7710>.
61. Han YH, Xia L, Song LP, Zheng Y, Chen WL, Zhang L, Huang Y, Chen GQ, Wang LS. Comparative proteomic analysis of hypoxia-treated and untreated human leukemic u937 cells. *Proteomics*. 2006;6(11):3262–74. <https://doi.org/10.1002/pmic.200500754>.
62. Liao SH, Zhao XY, Han YH, Zhang J, Wang LS, Xia L, Zhao KW, Zheng Y, Guo M, Chen GQ. Proteomics-based identification of two novel direct targets of hypoxia-inducible factor-1 and their potential roles in migration/invasion of cancer cells. *Proteomics*. 2009;9(15):3901–12. <https://doi.org/10.1002/pmic.200800922>.
63. Liu W, Shen SM, Zhao XY, Chen GQ. Targeted genes and interacting proteins of hypoxia inducible factor-1. *Int J Biochem Mol Biol*. 2012;3(2):165–78.
64. Mawhorter S, Yamani MH. Hypogammaglobulinemia and infection risk in solid organ transplant recipients. *Curr Opin Organ Transplant*. 2008;13(6):581–5. <https://doi.org/10.1097/MOT.0b013e3283186bbc>.
65. Jordan SC, Toyoda M, Kahwaji J, Vo AA. Clinical aspects of intravenous immunoglobulin use in solid organ transplant recipients. *Am J Transplant*. 2011;11(2):196–202. <https://doi.org/10.1111/j.1600-6143.2010.03400.x>.
66. Florescu DF, Kalil AC, Qiu F, Schmidt CM, Sandkovsky U. What is the impact of hypogammaglobulinemia on the rate of infections and survival in solid organ transplantation? a meta-analysis. *Am J Transplant*. 2013;13(10):2601–10. <https://doi.org/10.1111/ajt.12401>.
67. Consortium TU. UniProt: a worldwide hub of protein knowledge. *Nucleic Acids Res*. 2018;47(D1):506–15. <http://dx.doi.org/10.1093/nar/gky1049>.
68. Ritchie ME, Phipson B, Wu D, Hu Y, Law CW, Shi W, Smyth GK. Limma powers differential expression analyses for rna-seq and microarray studies. *Nucleic Acids Res*. 2015;43(7):47. <https://doi.org/10.1093/nar/gkv007>.
69. Yu G, Wang L, Han Y, He Q. clusterProfiler: an R package for comparing biological themes among gene clusters. *OMICS J Integr Biol*. 2012;16(5):284–287. <https://doi.org/10.1089/omi.2011.0118>.
70. Liberzon A, Birger C, Thorvaldsdottir H, Ghandi M, Mesirov JP, Tamayo P. The molecular signatures database (msigdb) hallmark gene set collection. *Cell Syst*. 2015;1(6):417–25. <https://doi.org/10.1016/j.cels.2015.12.004>.
71. Csardi G, Nepusz T. The igraph software package for complex network research. *InterJournal*. 2006;Complex Systems:1695.
72. Kanehisa M, Goto S. KEGG: Kyoto Encyclopedia of Genes and Genomes. *Nucleic Acids Res*. 2000;28(1):27–30. <http://dx.doi.org/10.1093/nar/28.1.27>.
73. Nishimura D. *BioCarta. Biotech Software & Internet Report*. 2001;2(3):117–120.
74. Fabregat A, Jupe S, Matthews L, Sidiropoulos K, Gillespie M, Garapati P, Haw R, Jassal B, Korninger F, May B, Milacic M, Roca CD, Rothfels K, Sevilla C, Shamovsky V, Shorsler S, Varusai T, Viteri G, Weiser J, Wu G, Stein L, Hermjakob H, D'Eustachio P. The Reactome Pathway Knowledgebase. *Nucleic Acids Res*. 2017;46(D1):649–55. <http://dx.doi.org/10.1093/nar/gkx1132>.
75. Wheeler B, Torchiano M. ImPerm: Permutation Tests for Linear Models. 2016. R package version 2.1.0. <https://CRAN.R-project.org/package=ImPerm>. Accessed 6 Mar 2020.
76. Hothorn T, Bretz F, Westfall P. Simultaneous inference in general parametric models. *Biom J*. 2008;50(3):346–63.

## Publisher's Note

Springer Nature remains neutral with regard to jurisdictional claims in published maps and institutional affiliations.

### Ready to submit your research? Choose BMC and benefit from:

- fast, convenient online submission
- thorough peer review by experienced researchers in your field
- rapid publication on acceptance
- support for research data, including large and complex data types
- gold Open Access which fosters wider collaboration and increased citations
- maximum visibility for your research: over 100M website views per year

At BMC, research is always in progress.

Learn more [biomedcentral.com/submissions](https://biomedcentral.com/submissions)

